NUREG/CR-3952

Sequoyah Equipment Hatch Seal Leakage

Final Report

Prepared by L. Greimann, F. Fanous, D. Bluhm

Ames Laboratory

Prepared for
U.S. Nuclear Regulatory Commission

NOTICE

This report was prepared as an account of work sponsored by an agency of the United States Government. Neither the United States Government nor any agency thereof, or any of their employees, makes any warranty, expressed or implied, or assumes any legal liability of responsibility for any third party's use, or the results of such use, of any information, apparatus, product or process disclosed in this report, or represents that its use by such third party would not infringe privately owned rights.

NOTICE

Availability of Reference Materials Cited in NRC Publications

Most documents cited in NRC publications will be available from one of the following sources:

1. The NRC Public Document Room, 1717 H Street, N.W.
   Washington, DC 20555
2. The Superintendent of Documents, U.S. Government Printing Office, Post Office Box 37082,
   Washington, DC 20013-7082
3. The National Technical Information Service, Springfield, VA 22161

Although the listing that follows represents the majority of documents cited in NRC publications, it is not intended to be exhaustive.

Referenced documents available for inspection and copying for a fee from the NRC Public Document Room include NRC correspondence and internal NRC memoranda; NRC Office of Inspection and Enforcement bulletins, circulars, information notices, inspection and investigation notices; Licensee Event Reports; vendor reports and correspondence; Commission papers; and applicant and licensee documents and correspondence.

The following documents in the NUREG series are available for purchase from the NRC/GPO Sales Program: formal NRC staff and contractor reports, NRC-sponsored conference proceedings, and NRC booklets and brochures. Also available are Regulatory Guides, NRC regulations in the *Code of Federal Regulations*, and *Nuclear Regulatory Commission Issuances*.

Documents available from the National Technical Information Service include NUREG series reports and technical reports prepared by other federal agencies and reports prepared by the Atomic Energy Commission, forerunner agency to the Nuclear Regulatory Commission.

Documents available from public and special technical libraries include all open literature items, such as books, journal and periodical articles, and transactions. *Federal Register* notices, federal and state legislation, and congressional reports can usually be obtained from these libraries.

Documents such as theses, dissertations, foreign reports and translations, and non-NRC conference proceedings are available for purchase from the organization sponsoring the publication cited.

Single copies of NRC draft reports are available free, to the extent of supply, upon written request to the Division of Technical Information and Document Control, U.S. Nuclear Regulatory Commission, Washington, DC 20555.

Copies of industry codes and standards used in a substantive manner in the NRC regulatory process are maintained at the NRC Library, 7920 Norfolk Avenue, Bethesda, Maryland, and are available there for reference use by the public. Codes and standards are usually copyrighted and may be purchased from the originating organization or, if they are American National Standards, from the American National Standards Institute, 1430 Broadway, New York, NY 10018.

NUREG/CR-3952
IS-4862

Sequoyah Equipment Hatch Seal Leakage

Final Report

Manuscript Completed: February 1985
Date Published: July 1985

Prepared by
L. Greimann, F. Fanous, D. Bluhm

Ames Laboratory
Iowa State University
Ames, IA 50011

Prepared for
Division of Engineering
Office of Nuclear Reactor Regulation
U.S. Nuclear Regulatory Commission
Washington, D.C. 20555
NRC FIN A4135-4

TABLE OF CONTENTS

LIST OF FIGURES

ACKNOWLEDGMENT

The authors would like to express their appreciation for three members of the U.S. Nuclear Regulatory Commission, Mr. Goutam Bagchi, Leader, Seismic Qualification Section; Mr. Vince Noonan, Chief, Equipment Qualifications Branch; and, Mr. Robert Wright, NRC Project Manager, for their help throughout the course of this work. Mr. Charles Hofmayer of Brookhaven National Laboratory and Mr. Tom Bridges of EG&G, Idaho, Inc., supplied information which was very useful for the conduct of this work. The authors also wish to acknowledge the able assistance of the project secretaries, Connie Bates and Beth Lott, for the word processor operations and the secretarial services associated with this project.

EXECUTIVE SUMMARY

Nuclear containments which will not leak significantly, i.e., beyond technical specifications, during a design accident may leak severely during a severe accident when the pressure increases beyond the design level. Small leaks which are visualized as occurring at local details may occur before complete vessel failure. As part of the NRC Containment Performance Working program, this study was undertaken to investigate the leakage-before-break potential of a typical equipment hatch seal. Buckling of the hatch door, large deformations and ovaling of the hatch sleeve are potential causes of mismatch at the sealing surface which can result in a leakage path.

Among the several plants being considered by the Containment Performance Working Group, the Sequoyah equipment hatch was selected. If penetrations effects are neglected, gross yielding of the 1/2-inch shell plate near the springline of the Sequoyah containment will occur at an internal pressure of between 50 and 60 psi.

The effect of an imperfection on the buckling strength of the hatch was first studied using an axisymmetric model of the hatch, containment and sleeve. A single axisymmetric imperfection lobe (cosine curve) was placed at the crown and adjacent to the seal. The buckling load for various values of the imperfection wave length and amplitude was calculated using the BOSOR5 code. The nonlinear behavior of the material was approximated by a piecewise linear relationship. The critical value of the imperfection wave length, amplitude and location was selected to be used in a three-dimensional finite element model.

The ANSYS finite element computer code was used to perform a three-dimensional finite element analysis of a portion of the containment with the sleeve/hatch assembly. The hatch system was modeled using flat triangular shell elements for the door, sleeve, containment, ring stiffeners and stringers. Prestressed bar elements were used to model the swing bolts and friction elements were employed to idealize the seal interface. Geometric and material nonlinear behavior were also included. The model was analyzed twice, using coefficients of friction of 0.6 and 0.3. In both analyses the pretension forces in the swing bolts were first applied and then the internal pressure was increased in increments as convergence was insured.

The results of the finite element analysis showed that a maximum of 0.9 inch of relative sliding occurred at the seal interface at 82 psi and the maximum relative rotation was 1-1/2 degrees. The buckling load was predicted to occur in the range of 85 to 90 psi, far above gross yielding of shell. Altnough buckling increased the relative seal motions, they remained sufficiently small to prevent leakage.

In conclusion, the Sequoyah equipment hatch should not leak before strains of several percent develop in the 1/2-inch containment shell plate near the springline, which occurs between 50 and 60 psi. In the unlikely event of hatch buckling, postbuckling deformations would not introduce leakage.

1. INTRODUCTION

1.1 Background

Nuclear containments are designed to prevent leakage of radioactive material. As the pressure and temperature increase during a severe accident, which is beyond the design level, the containment may reach a point where leakage begins to occur. There are at least two models used to characterize this leakage--the threshold model and the leak-before-break model.

In the threshold model, the containment is assumed to be leak-tight until certain pressure/temperature conditions are reached. At this point, a very large rupture or burst area is postulated and large quantities of fission products are released. Typically, the predicted threshold pressure is based upon a model of the containment shell which only permits such gross failure modes. Local discontinuities, e.g., penetrations, hatches, seals, are usually omitted from such models [1.1].

As an alternative model, the leak-before-break model is probably more realistic. In this model, it is hypothesized that small leak paths will develop as the containment is being pressurized at levels below the threshold. Hence, pressure is being released at earlier stages and the threshold pressure may never be reached. Typically, these small leaks are visualized as occurring at local details, e.g., penetrations, hatches, and seals which are often omitted from the threshold model.

The NRC has established a Containment Performance Working Group (CPWG), at the request of the Severe Accident Research Plan (SARP) Senior Review Group, to develop containment leakage models. Besides the containment loads aspect of this problem, this group is studying containment leakage in several categories. The current hypothesis of the group is that leakage will, most likely, begin at certain penetrations or other discontinuities (leak-before-break) and not by gross rupture of the containment shell. As a test for this hypothesis, the group is currently involved in quantifying predictions of the amount of leakage which may occur in six representative containments.

1.2 Objective

The objective of this particular work is to investigate the leak-before-break potential of a typical equipment hatch seal. The results will be incorporated into the work of the entire Containment Performance Working Group.

In the initial stages of the work, postbuckling and other large displacements of the equipment hatch shell itself were considered to be possible causes of leakage as local deformations distorted the sealing surface. As the project and communication with several others involved in similar work developed, another possibility became evident--ovaling of the penetration sleeve. That is, as the containment shell is

pressurized, circumferential forces in the containment tend to distort the hole and sleeve for the equipment penetration into an elliptical shape with a horizontal major axis. This distortion causes a mismatch of the sealing surface with leakage potential. This behavior is documented and described more fully herein.

2. EQUIPMENT HATCH DESCRIPTION

2.1 Hatch Selection

There are many different equipment hatch configurations in existing containments. Since an initial consideration was postbuckling displacement, a hatch under compression was selected (pressure seating) as opposed to a hatch in tension (pressure unseating). Again, since buckling was important, it was decided to select a hatch with the most likely possibility of buckling, i.e., a large r/t value. From the six plants being studied by the Containment Performance Working Group, the Sequoyah equipment hatch was selected.

2.2 Geometry and Materials

The Sequoyah equipment hatch is located on Azimuth 285° at Elevation 741' 1 1/2" of the containment (Fig. 2.1). More geometric details of the containment in the vicinity of the hatch are shown in Figs. 2.2, 2.3 and 2.4. Of particular interest in these figures are:

(1) The containment shell is 1/2 inch thick just below the upper springline. Previous studies [2.1] using axisymmetric (threshold type) models of the Sequoyah containment which neglect penetrations and other nonsymmetric discontinuities, predict gross shell yielding in the 1/2 inch plate at a static pressure between 50 and 60 psi. (The variation in this value is the result of different approaches by the different investigations.)

(2) There is 5/8 inch shell plate in the immediate vicinity of the equipment hatch penetration (Fig. 2.2). The local plate thickness of 1-1/2 inch is presumably used to satisfy the ASME area replacement rule.

(3) The sleeve length between the containment wall and the sealing surfaces is only 14.5 inches at the horizontal diameter of the sleeve. This distance is quite short and, as will be seen, couples the containment deformations to the deformations at the sealing surface.

(4) The actual containment in the upper right quadrant of the hatch region is shown in Fig. 2.2, except a ring actually located at Elevation 740' 6 5/8" was moved to the hatch centerline to introduce symmetry. The containment in the remaining three quadrants is not symmetrical, e.g., the 5/8 inch plate does not exist in the same locations in the other quadrants. The assumed quarter symmetry of the 5/8 inch plate will provide an upper bound to the sleeve movements.

Shell geometric imperfections have a significant effect on buckling strength. Particularly for spherical shells under external pressure, small deviations from perfect sphericity greatly reduce the buckling

strength below classical buckling theory. Figure 2.5 illustrates the ASME tolerance criteria on shell imperfections [2.2]. For the Sequoyah hatch, the maximum deviation from a perfect circular arc, e, is permitted to be one shell thickness (3/4 inch) over a chord length of 67 inches.

The details of the seals as furnished by TVA are shown in Fig. 2.6. Compression set values (ASTM D 395) for typical temperature/radiation loadings are also listed.

The containment steel is A516, Grade 60 with a specified minimum yield of 32 ksi. Actual mill test yield strengths for typical plates with the various thicknesses are listed in Fig. 2.7. The effect of temperature on yield strength was not considered. In the fabrication process, flat steel plates are deformed to fit the singly and doubly curved surfaces of the containment and hatch. Even though the plates and the subsequent welding may be stress-relieved, the proportional limit of the material is seldom restored to its virgin value near the yield point. This has a significant effect on the buckling strength of steel components because the material tangent modulus is reduced. In lieu of knowing the residual stress pattern, this effect can be approximated by using an effective stress-strain curve with a proportional limit below the yield strength [2.4, 2.5]. For the present case, the proportional limit will be taken as one-half yield which approximates residual stresses of the order of one-half yield. For each thickness, the stress-strain curve is approximated by a modified Ramberg-Osgood equation [2.2] with a strain hardening exponent n of five (Fig. 2.7). For purposes of the following analysis, this curve is approximated by a piecewise linear curve.

3. IMPERFECTION STUDY

As mentioned previously, imperfections in the spherical cap hatch can have a large effect on its buckling and, hence, postbuckling behavior. To study this effect in an economical manner, an axisymmetric model of the hatch and sleeve was developed for BOSOR5 [3.1]. Since the model is axisymmetric, the cylindrical containment was approximated by a portion of a sphere (Fig. 3.1). No relative motion was permitted at the sealing surface. The effect of these assumptions on the buckling strength is not clear. Intuitively, the combined effect of the tension in the equivalent sphere and the nonsliding sealing surface may displace the hatch boundaries outward, reducing its buckling strength. It is exactly such uncertainties in this model which encourage the development of a more complete three-dimensional model. However, a first approximation as to the relative effect of an imperfection can be studied with this simpler model.

A single axisymmetric imperfection lobe (cosine curve) was placed at the crown (Fig. 3.2) and adjacent to the flange (Fig. 3.3). BOSOR5 was executed to calculate the buckling load for various values of the imperfection wave length, L_o, and amplitude. The resulting buckling pressures are plotted in Figs. 3.4 and 3.5, respectively. The critical buckling length for classical elastic buckling of a complete perfect sphere is approximately [3.2]

$$L_{cr} \approx 3.5\sqrt{rt} = 47 \text{ in.} \qquad (3.1)$$

Figure 3.4 illustrates that the wave length of the crown imperfection, which minimizes the buckling strength of the Sequoyah hatch, is about 35 inches. Note the hatch is actually closer to a spherical cap than a complete sphere. The length of the (axisymmetric) imperfection adjacent to the flange has little effect on buckling strength. As expected, Fig. 3.5 confirms that an increasing imperfection amplitude decreases buckling strength, especially for an imperfection at the flange. Note again that the maximum permitted value of e for the Sequoyah hatch is 3/4 inch (see Sec. 2.3).

The "design" buckling pressure for the hatch as calculated from the ASME Code, Case N-284 [3.3] is 50 psi. (In terms of Case N-284, the capacity reduction factor is 0.146 ($M = 240/\sqrt{(240)(0.75)} = 17.9$), the classical elastic buckling pressure of a perfect sphere is 343 psig and the plasticity reduction factor is 1.0, i.e., elastic buckling.) In Code Case N-284, the effect of the spherical cap boundary condition is treated as an imperfection and incorporated into the capacity reduction factor through the nondimensional length M. The design buckling pressure for the spherical cap could be as high as 99 psig [3.4] depending upon the capacity reduction factor. The 50 psi value is shown in Fig. 3.5.

For the subsequent three-dimensional analysis, a single imperfection lobe was used with a length, L_o, of 47 inches and a deviation for

perfect circularity, e, of 3/4 inch (Fig. 3.6). The imperfection was also assumed to be L_p in the circumferential direction, on the basis that this shape will be sympathetic with the elastic buckling mode in which n lobes form around the circumference. (BOSOR5 indicated n was about 8 for this case [3.5].) The imperfection was located near the flange to maximize its effect on possible distortion at the sealing surface. In anticipation of the possible ovaling effect (Sec. 1.2), compression in the hatch will be largest in the vertical direction. Hence, the imperfection was placed on a vertical diameter.

4. THREE-DIMENSIONAL ANALYSIS

4.1 Model

A three-dimensional finite element model of the Sequoyah equipment hatch was constructed for the ANSYS [4.1] computer program. ANSYS is a general purpose finite element computer program with extensive pre- and postprocessing capability. The geometric and material nonlinear analysis capabilities of ANSYS were used in this model. The geometric and material properties presented in Sec. 2.2 and the imperfection in Fig. 3.6 were incorporated into the model. One-quarter symmetry is assumed about the hatch vertical and horizontal diameters, as suggested in Fig. 2.2, even though the containment is only approximately symmetrical. Note that the quarter-symmetry model precludes asymmetric buckling.

Symmetry boundary conditions were used in the plane of the vertical and horizontal diameters of the hatch. The model is extended only 20 degrees circumferentially from the meridional plane through the center of the hatch (Fig. 2.2). (This certainly represents a minimum. The effect of this arbitrary boundary was not studied.) Symmetry boundary conditions are also used on this boundary. The top of the model is constrained to move uniformly vertically, i.e., the top of the model remains a plane section.

The mesh in the hatch and sleeve was laid out such that the maximum element dimension was less than $\sqrt{rt}/2$ (6.7 inch for the hatch and 9.5 inch for the sleeve). Flat triangular shell elements were used (STIF48 in ANSYS). The elements in the containment shell are noticeably larger than this guideline ($\sqrt{rt}/2$ of 16 inch), but sufficiently small to approximate its membrane behavior. Rings and stringers were also modeled by shell elements. Figure 4.1 and 4.2 are plots of the finite element mesh from outside and inside the containment, respectively (915 elements, 541 nodes).

The swing bolts which are pretensioned to hold the hatch against the sealing surface (Fig. 2.4) were included in the model as uniaxial, pretensioned bar elements (STIF8). The swing bolts are rigidly connected to the middle surface of the sleeve shell and the hatch flange at nodes corresponding to the bolt locations.

The material model is the von Mises yield surface with the Prandtl-Reuss flow rule with isotropic strain hardening. The piecewise linear approximation to the uniaxial stress-strain curve is illustrated in Fig. 2.7.

The interface between the flange and the sleeve is modeled using interface elements (STIF 52) which have friction and opening capability (Fig. 4.3). Normal to the interface, the element is very stiff in compression and very flexible in tension. (Infinite and zero stiffnesses introduce numerical problems.) Tangential to the interface, the element permits relative sliding if the tangential force exceeds the

normal (compressive) force multiplied by the coefficient of friction. Equilibrium for the interface elements is taken about the undeformed position. Hence, these elements, although they do simulate the frictional behavior, only approximate the large displacement behavior at the seal interface. Two interface elements are used at each nodal meridian of the sleeve--one on the inside and one on the outside of the sleeve.

Such an arrangement permits rotational and sliding discontinuities at the seal interface. (The results to follow illustrate this.) Two different coefficients of friction, 0.6 and 0.3, were used in the analysis of the hatch model. A coefficient of friction of 0.6 represents the clean steel on steel case [4.2].

4.2 Loads and Execution

The finite element model described in the previous section was loaded to correspond to internal pressure on the containment, i.e., pressure on the inside face of the appropriate elements and a vertical load at the top of the model corresponding to the meridional membrane stress resultant in the containment. Two different analysis approaches available in the ANSYS Code were used to analyze the hatch model. A static analysis was performed with the 0.6 coefficient of friction case, while a "slow-dynamic" analysis was used in conjunction with the 0.3 friction coefficient. In both approaches, the prestress in the swing bolts was first applied (25 kips/bolt which is about 1/4 the yield strength) and then the pressure inside the containment was applied.

In the static analysis, the pressure was increased in increments, typically 5 psi. After each increment in pressure was applied, a sufficient number of iterations was run to permit convergence to the nonlinear solution. Convergence criteria were: (1) the change in displacement between consecutive iterations must be less than 0.1 inch and (2) the change in plastic strain divided by the yield strain be less than 0.1. Beyond 80 psi, these criteria were reduced to 0.05 and 0.05, respectively. Through the 82 psi load level, the solution required iterations which used about 55 cpu hours on a VAX 11/780. When the pressure was increased to 84 psi, a zero-stiffness condition occurred, indicating the hatch had buckled at the imperfection. A couple unsuccessful attempts were made to follow the postbuckling behavior using the traditional static analysis.

In an attempt to track the postbuckling behavior with a physically, more realistic analysis, the "slow dynamic" analysis suggested in [4.1] was used for the 0.3 coefficient of friction case. In principle the method is more attractive because the actual buckling process is dynamic. A high damping ratio is used to minimize the vibration response. Physically, this would correspond to placing the hatch in a viscous fluid during pressurization. The pressure in this analysis was increased linearly over a rise time larger than several times the structure natural period (about 1 psi per second). The integration

time increments were initially quite large (1 second) as the structure behaved linearly and the high damping produced an essentially static response. As material and geometric nonlinearities began to dominate the problem, the time steps were successively cut in half. For example, a time step of 0.125 seconds was used at 82 psi. This solution required about 70 cpu hours to reach the 82 psig level. At this point, the pressure was increased to 85 psi as a step function and 24 time increments of 0.01 second were run but no buckling occurred. Since the postbuckling shape and not necessarily the buckling pressure were desired, the pressure was stepped to 90 psi and the solution was continued for 100 time steps. During these steps, the time increment size was increased from 0.01 to 0.1 seconds. An additional 75 cpu hours of computer time were required.

4.3 Results

4.3.1 Prebuckling Results

Typical strain and displacement results are presented in this section. Figure 4.4 will be used to reference the location of the points of interest. Figure 4.5 is a plot of the radial displacement at the center of the hatch, A, the center of the imperfection, B, and the 5/8-inch containment shell plate, C. The displacement at B is the maximum in the model. Strains of interest are plotted in Fig. 4.6. The maximum strain in the hatch occurs at the surface in the imperfection, B. Of all the membrane strains in the containment, the maximum occurs in the 5/8 inch plate near C. The maximum membrane strain in the entire model occurs in the horizontal direction at the top of the sleeve, D, just outside the containment. Most of the differences between the results for the 0.3 and 0.6 friction cases are caused by the difference in the analysis techniques.

The distortions at the sealing surface can be visualized by examining the deformed shapes at the vertical and horizontal symmetry planes of the hatch, Fig. 4.7 and 4.8, respectively. These figures are plotted for the 0.3 coefficient of friction at 82 psig. Displacements are drawn at an exaggerated scale in these figures. The inset figures in each of these plots are drawn to scale and illustrate the translation and rotation relative to the flange and the flange grooves. The swing bolts lose their prestress at about 70 psig. These figures and Fig. 4.9 illustrate the ovaling effect, i.e., the forces in the containment shell tend to distort the sleeve into an ellipse. If the frictional forces at the sealing surface where zero, the sleeve would become elliptical and the hatch flange would remain circular with a uniform outward radial motion. This mismatch in shapes causes sliding and rotation at the sealing surface. As will be illustrated in the following paragraph, friction reduces this mismatch, i.e., tends to force the two surfaces to move together, but it does not eliminate it.

Figures 4.10 and 4.11 are plots of the vertical displacement in the vertical symmetry plane, F, and the horizontal displacement in the horizontal symmetry plane, G, respectively, at the sealing surface.

Down is positive in Fig. 4.10 and to the right is positive in Fig. 4.11. The difference in the displacement for the sleeve and the flange represent the slip at the seal surface. Notice that, as expected, the slip is larger when the coefficient of friction was reduced to 0.3. In this case, the differences in slip are caused by the differences in the coefficient of friction and not the different analysis techniques. Figures 4.12 and 4.13 present the rotations at the sealing surface in the vertical and horizontal symmetry planes, respectively. Positive rotations are shown in the inset. Again, the distance between the two curves represents the relative rotation of the two surfaces. The relative rotation was not much affected by the change in the coefficient of friction.

4.3.2 Postbuckling Results

When the pressure was stepped to 90 psig, buckling occurred as the imperfection grew. Figure 4.14 illustrated various stages of the deformed shape during buckling. The displacements and original geometry are plotted to the same scale. As complete snap-through occurs, the relative translation and rotation at the sealing surface increases to 2.4 inches and 2.7 degrees, respectively, as illustrated by the inset figures of Fig. 4.14. Note that the one-quarter symmetry assumption in the model precludes a nonsymmetric buckling pattern. Even with these seal displacements, leakage is unlikely [4.4]. Large strains associated with the snap-through (up to 8.25 percent) could, of course, cause material separation and subsequent leakage. However, the 90 psig associated with this process would not be reached because general containment shell failure would occur below this at about 60 psig (Item (1) in Sec. 2.2).

4.4 Summary Observations

The maximum strain in the model at 82 psig, for both friction cases, is about 0.014 in the penetration sleeve (Fig. 4.4). Although this strain is probably well below the ultimate strain for the ductile steel used in the containment, the possibility exists that localized plane strain conditions and local flaws may initiate a leakage point. Elastic-plastic fracture mechanics principles could usefully be applied here [4.3].

The maximum relative motion at the seal surface at 82 psig are 0.9 inch sliding and 1 1/2 degree relative rotation for the 0.3 coefficient of friction. Postbuckling displacements increased this value to 2.4 inches and 2.7 degrees, respectively. With this small amount of displacement of the seals, leakage is unlikely [4.4].

5. SUMMARY

5.1 Summary

Nuclear containments which will not leak significantly, i.e., beyond technical specifications, during a design accident may leak severely during a severe accident when the pressure increases beyond the design level. Small leaks which are visualized as occurring at local details may occur before complete vessel failure. As part of the NRC Containment Performance Working program, this study was undertaken to investigate the leak-before-break potential of a typical equipment hatch seal. Buckling of the hatch door, large deformations and ovaling of the hatch sleeve are potential causes of mismatch at the sealing surface which can result in a leakage path.

Among the several plants being considered by the Containment Performance Working Group, the Sequoyah equipment hatch was selected. If penetrations effects are neglected, gross yielding of the 1/2-inch shell plate near the springline of the Sequoyah containment will occur at an internal pressure of between 50 and 60 psi.

The effect of an imperfection on the buckling strength of the hatch was first studied using an axisymmetric model of the hatch, containment and sleeve. A single axisymmetric imperfection lobe (cosine curve) was placed at the crown and adjacent to the seal. The buckling load for various values of the imperfection wave length and amplitude was calculated using the BOSOR5 code. The nonlinear behavior of the material was approximated by a piecewise linear relationship. The critical value of the imperfection wave length, amplitude and location was selected to be used in a three-dimensional finite element model.

The ANSYS finite element computer code was used to perform a three-dimensional finite element analysis of a portion of the containment with the sleeve/hatch assembly. The hatch system was modeled using flat triangular shell elements for the door, sleeve, containment, ring stiffeners and stringers. Prestressed bar elements were used to model the swing bolts and friction elements were employed to idealize the seal interface. Geometric and material nonlinear behavior were also included. The model was analyzed twice, using coefficients of friction of 0.6 and 0.3. In both analyses the pretension forces in the swing bolts were first applied and then the internal pressure was increased in increments as convergence was insured.

The results of the finite element analysis showed that a maximum of 0.9 inch of relative sliding occurred at the seal interface at 82 psi and the maximum relative rotation was 1-1/2 degrees. The buckling load was predicted to occur in the range of 85 to 90 psi, far above gross yielding of the shell. Although buckling increased the relative seal motions, they remained sufficiently small to prevent leakage.

5.2 Conclusions

In conclusion, the Sequoyah equipment hatch should not leak before strains of several percent develop in the 1/2-inch containment shell plate near the springline, which occurs between 50 and 60 psi. In the unlikely event of hatch buckling, postbuckling deformations would not introduce leakage.

5.3 Recommendations

Some of the items which were not included in this study which could be looked at in the future include other hatch imperfections, different friction coefficients and other pretensions in the swing bolts. The analysis methods should continue to be calibrated with existing experimental results, many of which have been published, e.g., shell buckling, pressure vessel experiments. The behavior and the seals with flange separation and rotation needs more study. The effect and temperature gradients on displacements at the seal surface could be important.

High strains in the sleeve, near the containment, should be investigated further. As pressure is increased, material separation will most likely begin at these high strain locations. The potential size of such a path should be studied. Several other penetrations with possibly higher strains should also be considered.

6. REFERENCES

1.1 Greimann, L, Fanous, F., and Bluhm, D., "Containment Analysis Techniques, A State-of-the-Art Summary," Report to Sandia National Laboratory, October 1983.

2.1 Greimann, L., et. al, "Reliability Analysis of Containment Strength, Sequoyah and McGuire Ice Condenser Containments," NUREG/CR-1891, August 1982.

2.2 ASME Boiler and Pressure Vessel Code, Section III, Division I, Subsection NE, Paragraph NE-4220, 1982.

2.3 Desai, C.S. and Wu, T.H., "A General Function for Stress-Strain Curves," Numerical Methods in Geometrics, ASCE, 1976.

2.4 Brockenbrough, R.L. and Johnston, B.G., Steel Design Manual, U.S. Steel, Pittsburgh, PA, 1974, pg. 47.

2.5 Salmon, C.G. and Johnson, J.E., Steel Structures Design and Behavior, 2nd Edition, Harper and Row, New York, 1980, pg. 263.

3.1 Bushnell, D., "BOSOR5, A Program for Buckling of Elastic-plastic Complex Shells of Revolution Including Large Deflections and Creep," Structural Mechanics Laboratory, Lockheed Missile and Space Co., Palo Alto, CA, 1974.

3.2 Brush, D.O. and Almorth, B.O., Buckling of Bars, Plates, and Shells, McGraw-Hill, New York, 1975, Chap. 7.

3.3 ASME Boiler and Pressure Vessel Code, Case N-284, "Metal Containment Shell Buckling Design Methods," Supplement #2 to Nuclear Code Case Book, 1980.

3.4 Baker, H., et. al, "Shell Analysis Manual," NASA CR-0912, April 1968.

3.5 Wackel, N., Jullien, J.F. and Ledermann, P., "Experimental Studies of the Instability of Cylindrical Shells with Initial Imperfections," Recent Advances in Nuclear Component Testing and Theoretical Studies in Buckling, PVP-Vol. 89, ASME, June 17-21, 1984.

4.1 ANSYS Engineering Analysis System, User's Manual and Theoretical Manual, Swanson Analysis Systems, Inc., Houston, PA, 1984 (Version 4.1C).

4.2 Handbook of Chemistry and Physics, 41 Edition, Chemical Rubber Publishing Co., Cleveland, 1960, pg. 2152.

4.3 Idelsohn, S.R., et. al, "Failure Internal Pressure of Spherical Steel Containments," Second Workshop on Containment Integrity, Washington, D.C., June 1984.

4.4 Barnes, B.L., "Containment Penetration Elastomer Seal Test," Second Workshop on Containment Integrity, Washington, D.C., June 1984.

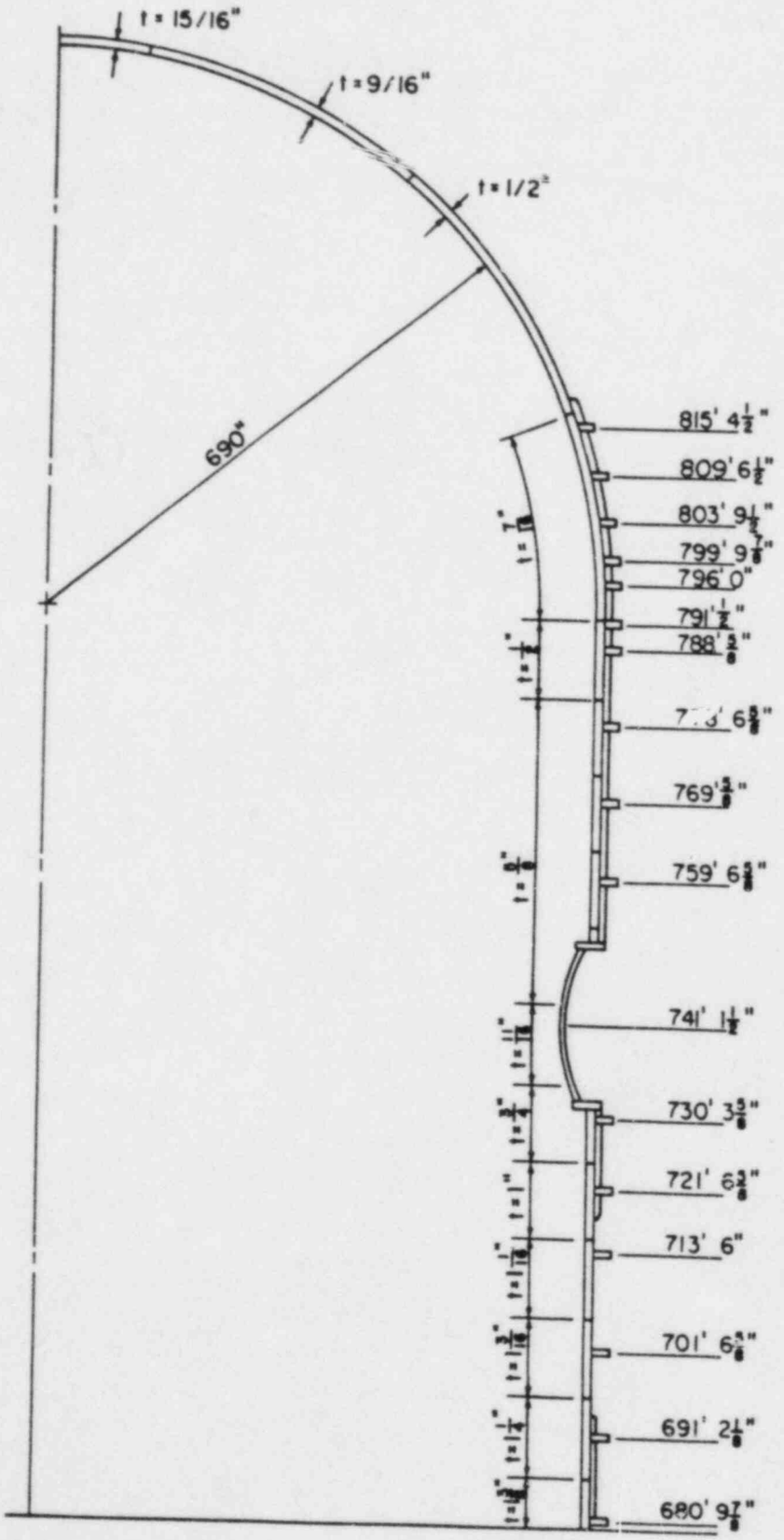

Figure 2.1 Sequoyah Containment - Azimuth 285°

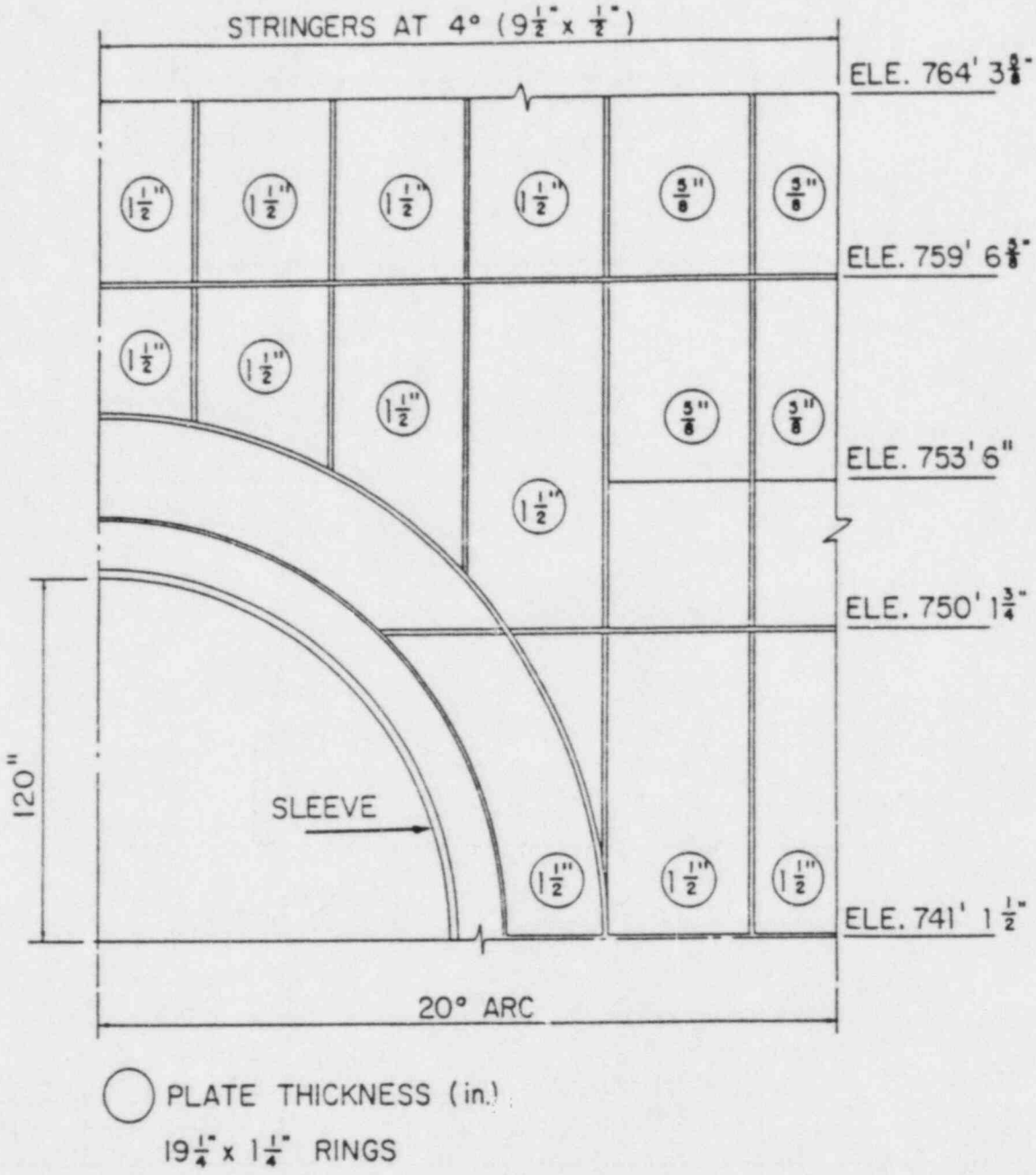

Figure 2.2 Sequoyah Containment Shell Plate Thicknesses

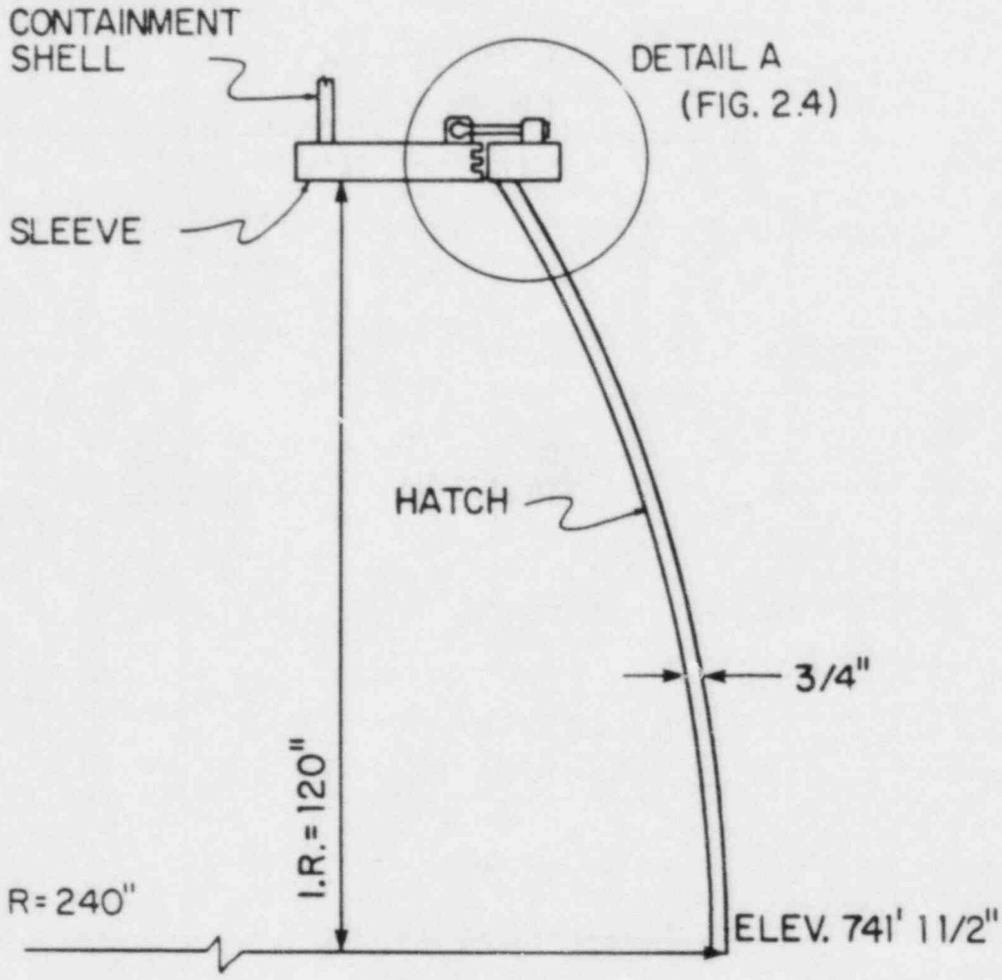

Figure 2.3 Sequoyah Equipment Hatch Elevation

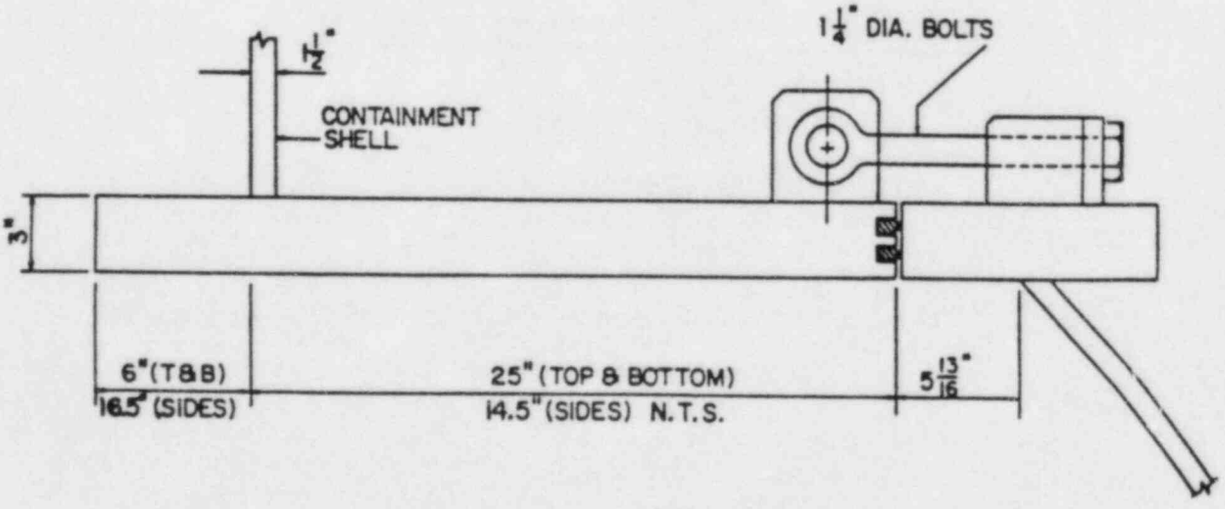

Figure 2.4 Detail A - Sequoyah Equipment Hatch

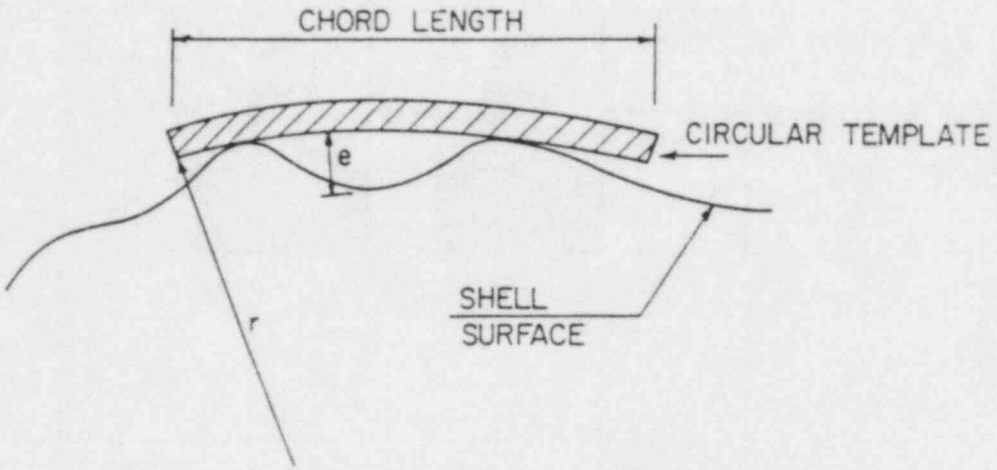

CHORD LENGTH = TWICE THE ARC LENGTH

ARC LENGTH = FIG. 4221.2.2 ASME CODE, SUBSECTION NE

e = DEVIATION FROM TRUE SHAPE
FIG. 4221.2.1 ASME CODE

r = INSIDE OR OUTSIDE SHELL RADIUS

Figure 2.5 ASME Tolerance for Shells

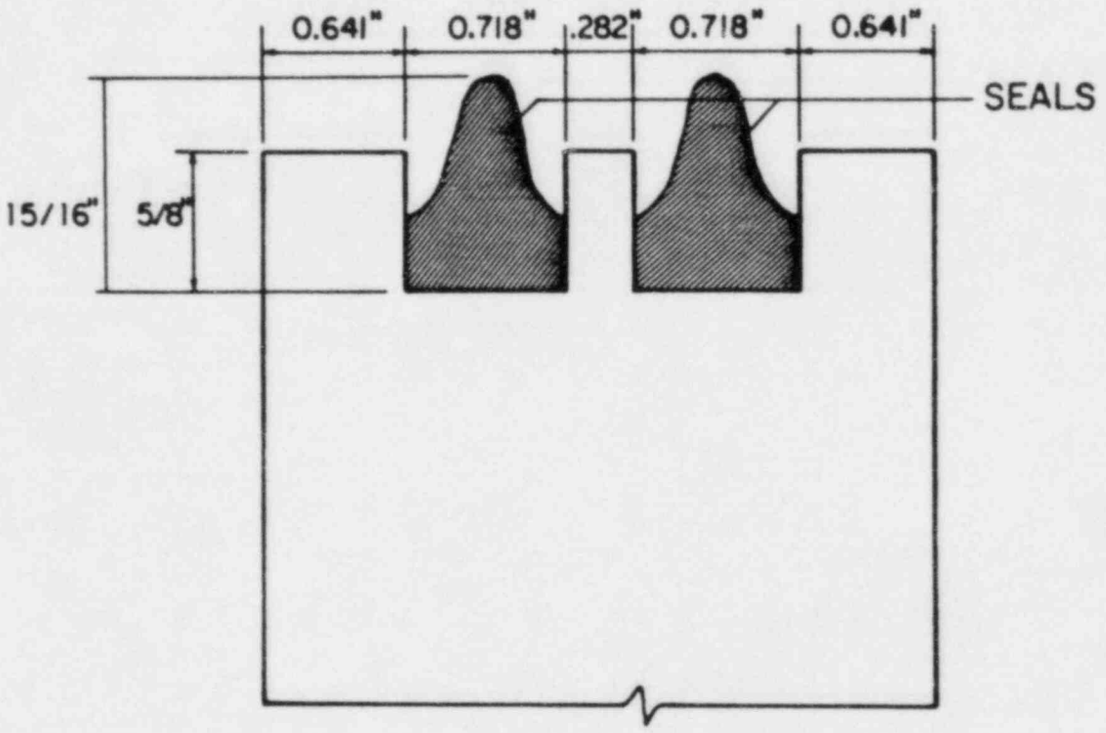

PRESRAY EPDM COMPOUND E 603

	COMPRESSION SET
158°F FOR 22 HRS	14.1 %
7×10^5 RADS AT 120°F FOLLOWED BY 10^8 RADS AT 250°F FOR 72 HRS	13.1 %

Figure 2.6 Seal Configuration

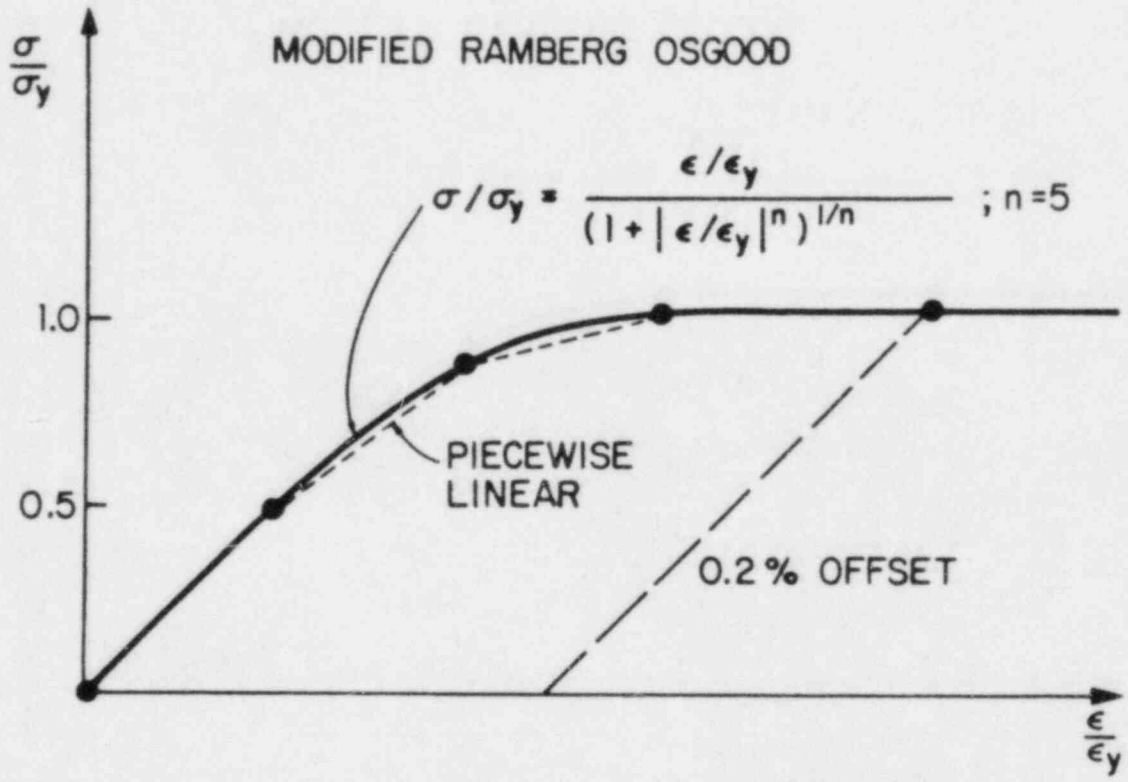

A 516 Gr. 60

PL THICKNESS (in.)	σ_y (KSI)
$\frac{5}{8}$"	49.2
$\frac{3}{4}$"	43.7
$1\frac{1}{4}$"	45.5
$1\frac{1}{2}$"	46.1
3"	40.8

Figure 2.7 Idealized Stress-Strain Curve for Steel

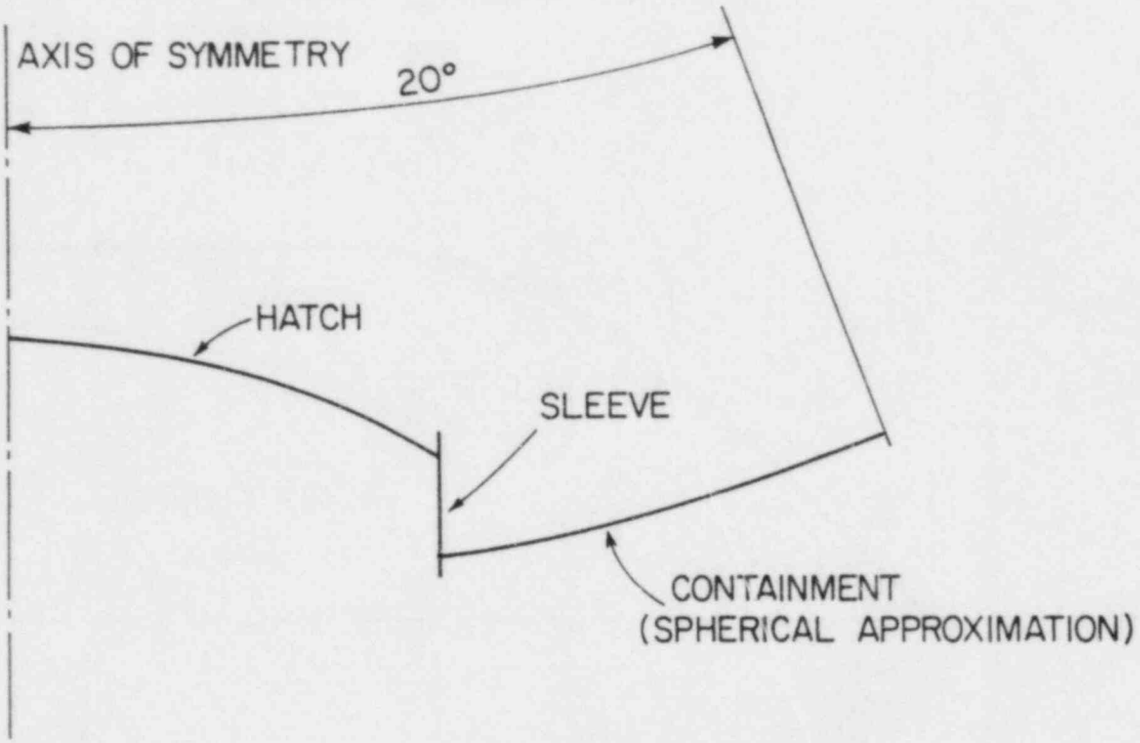

Figure 3.1 BOSOR5 Axisymmetric Finite Difference Model

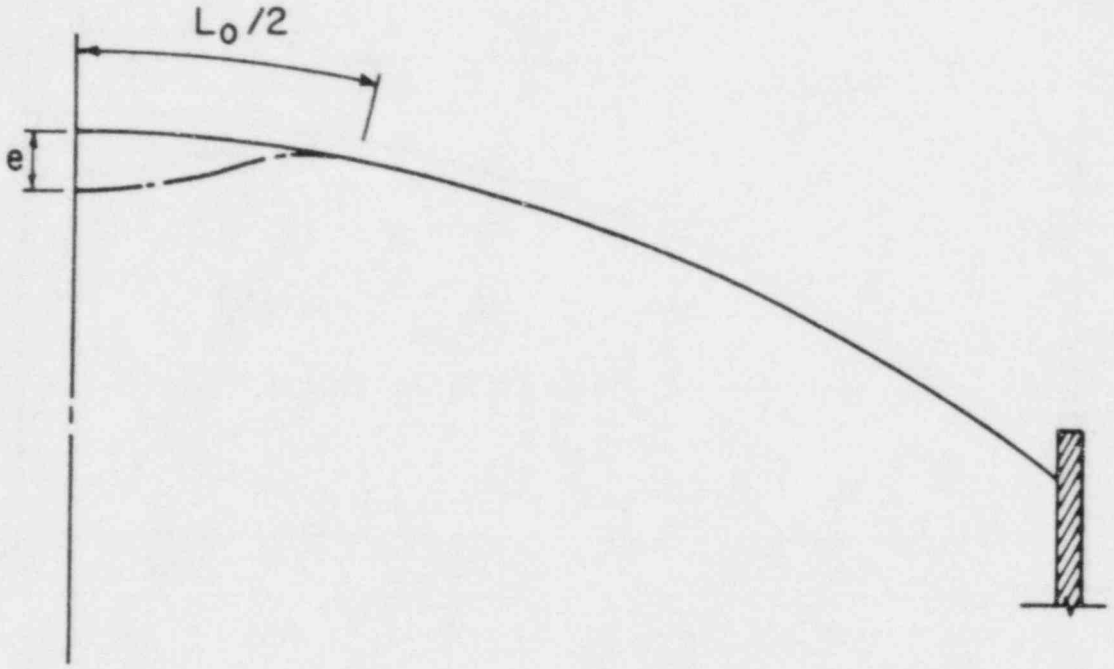

Figure 3.2 Idealized Imperfection at Crown

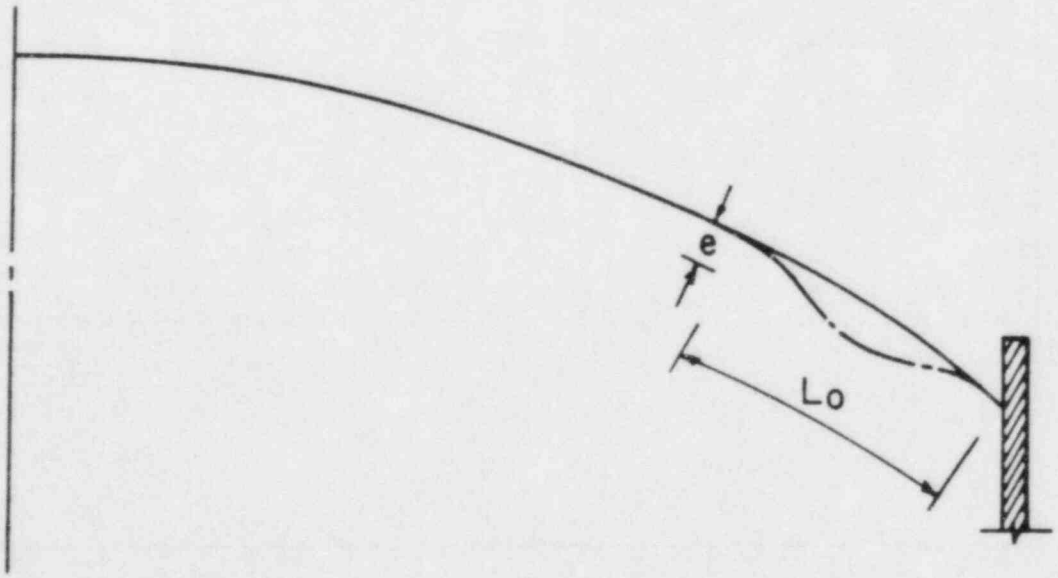

Figure 3.3 Idealized Imperfection at Flange

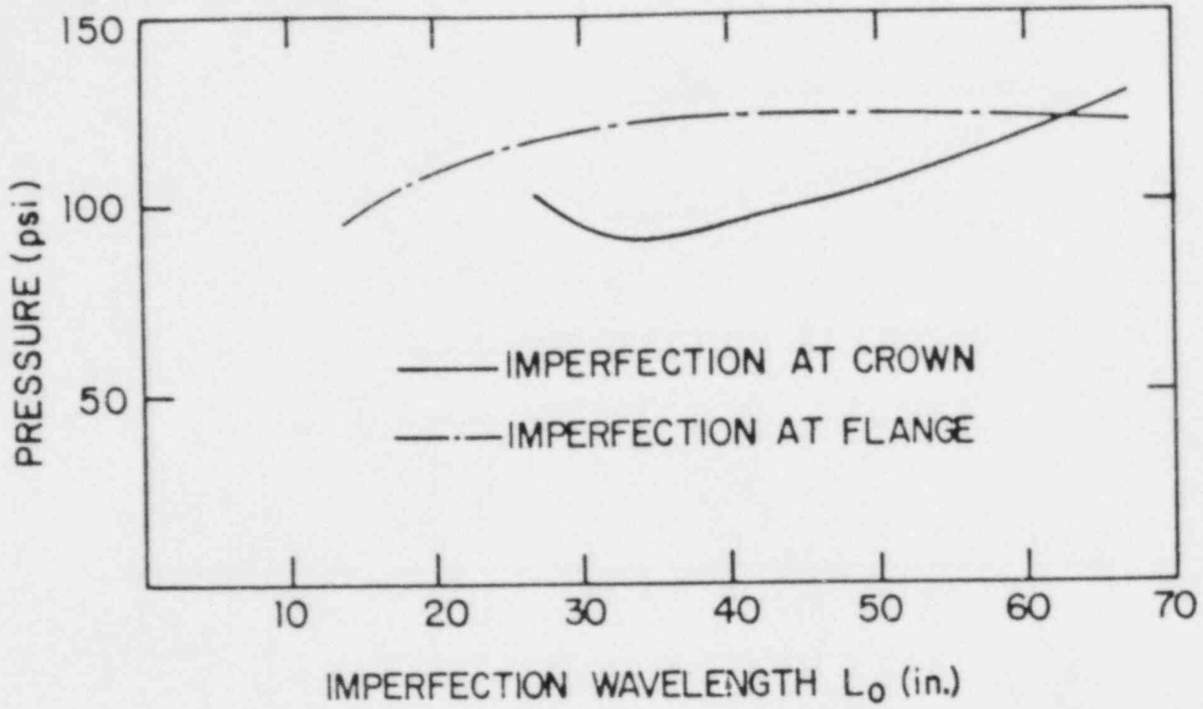

Figure 3.4 Influence of Imperfection Wavelength (Imperfection Amplitude = .75 in.)

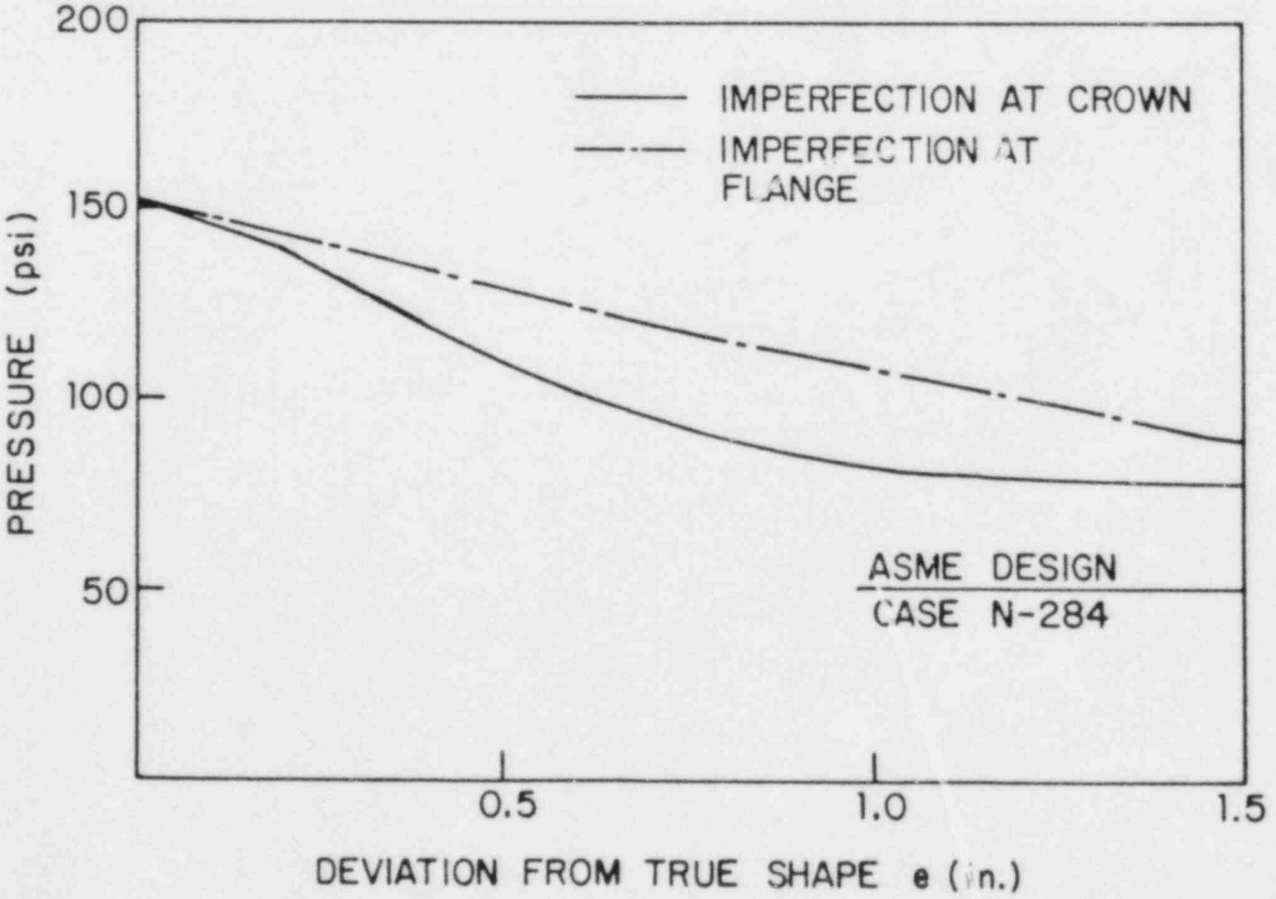

Figure 3.5 Influence of Imperfection Magnitude (Imperfection Wavelength = 47 in.)

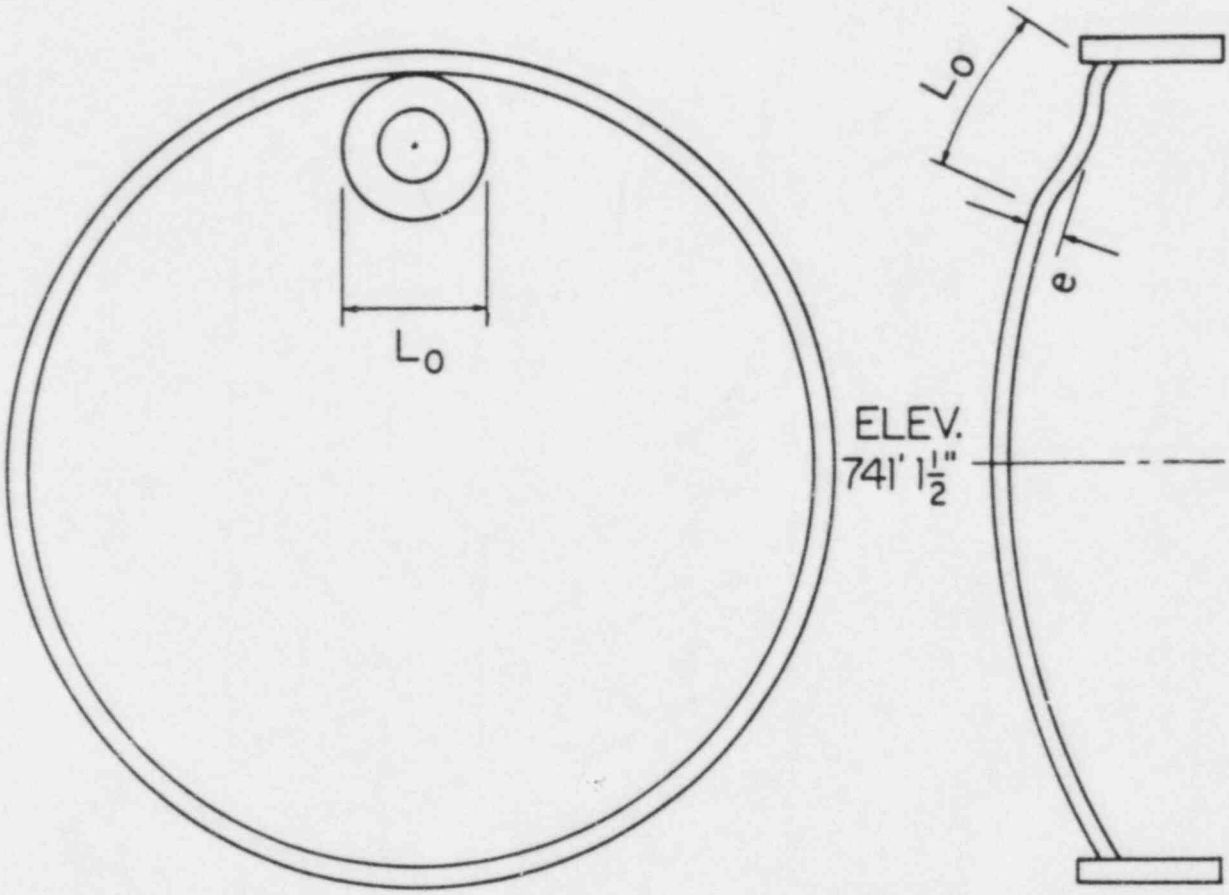

Figure 3.6 Assumed Imperfection for Three-Dimensional Analysis

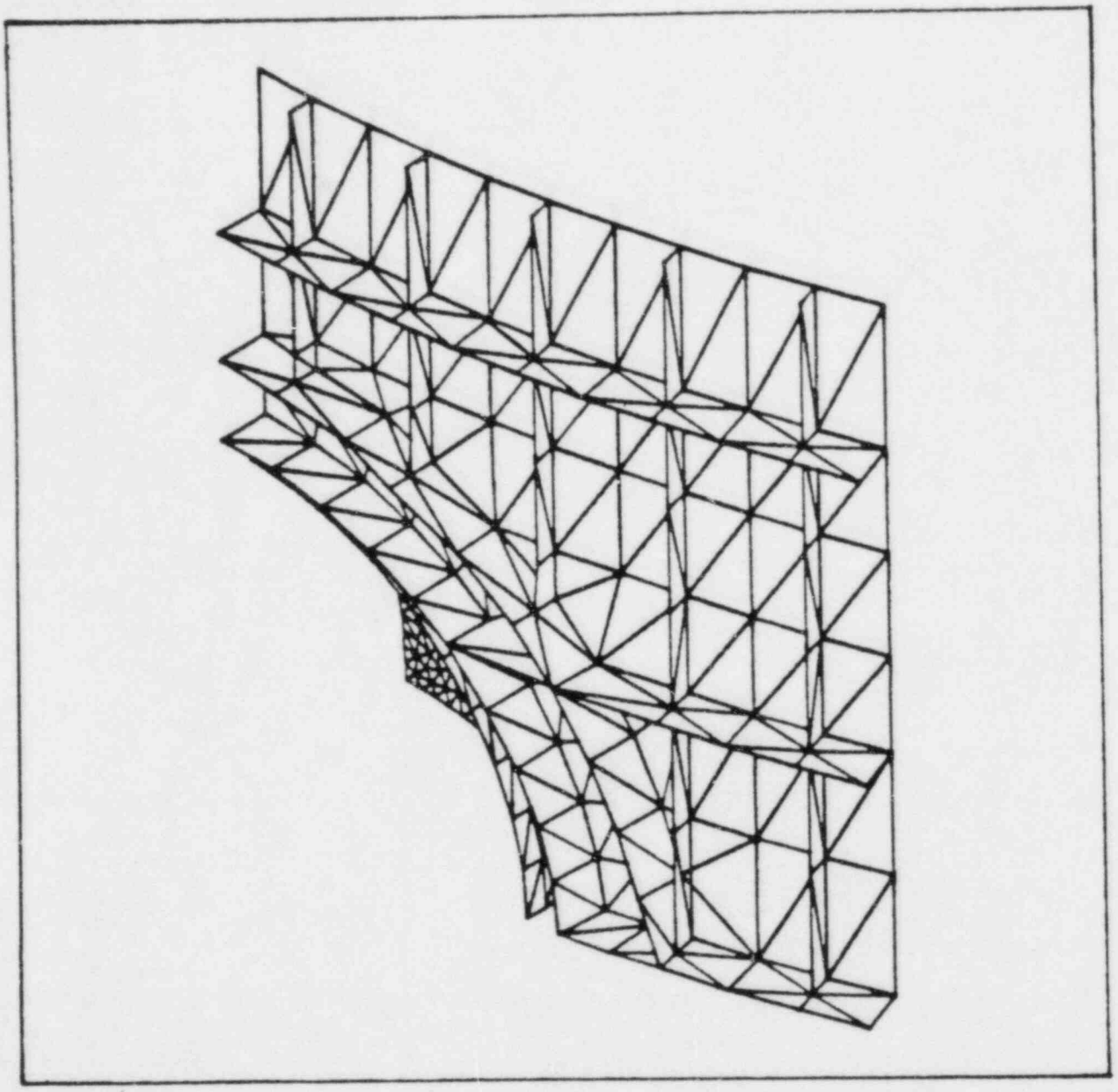

Figure 4.1 Sequoyah Containment Equipment Hatch-Outside View

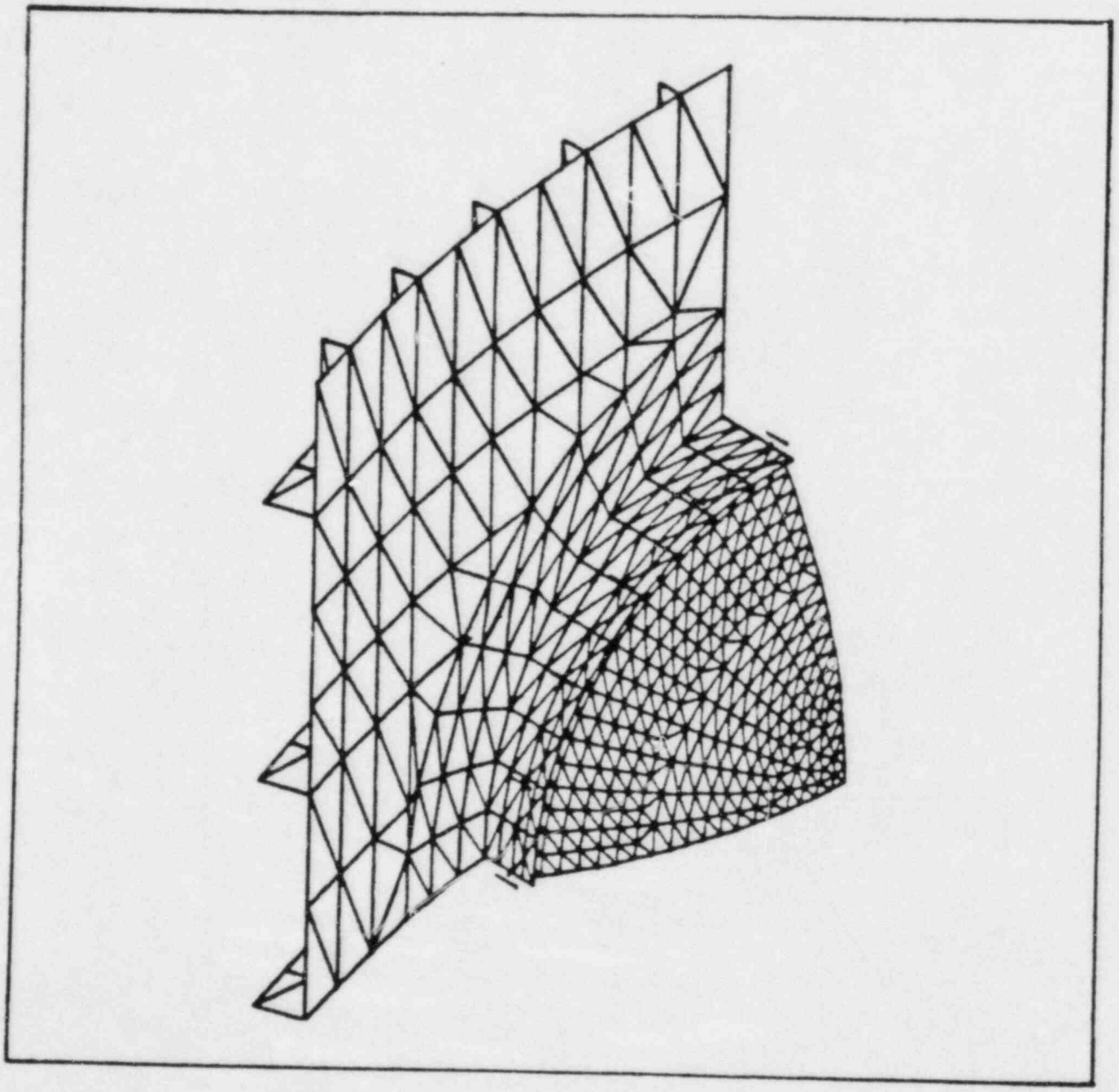

Figure 4.2 Sequoyah Containment Equipment Hatch-Inside View

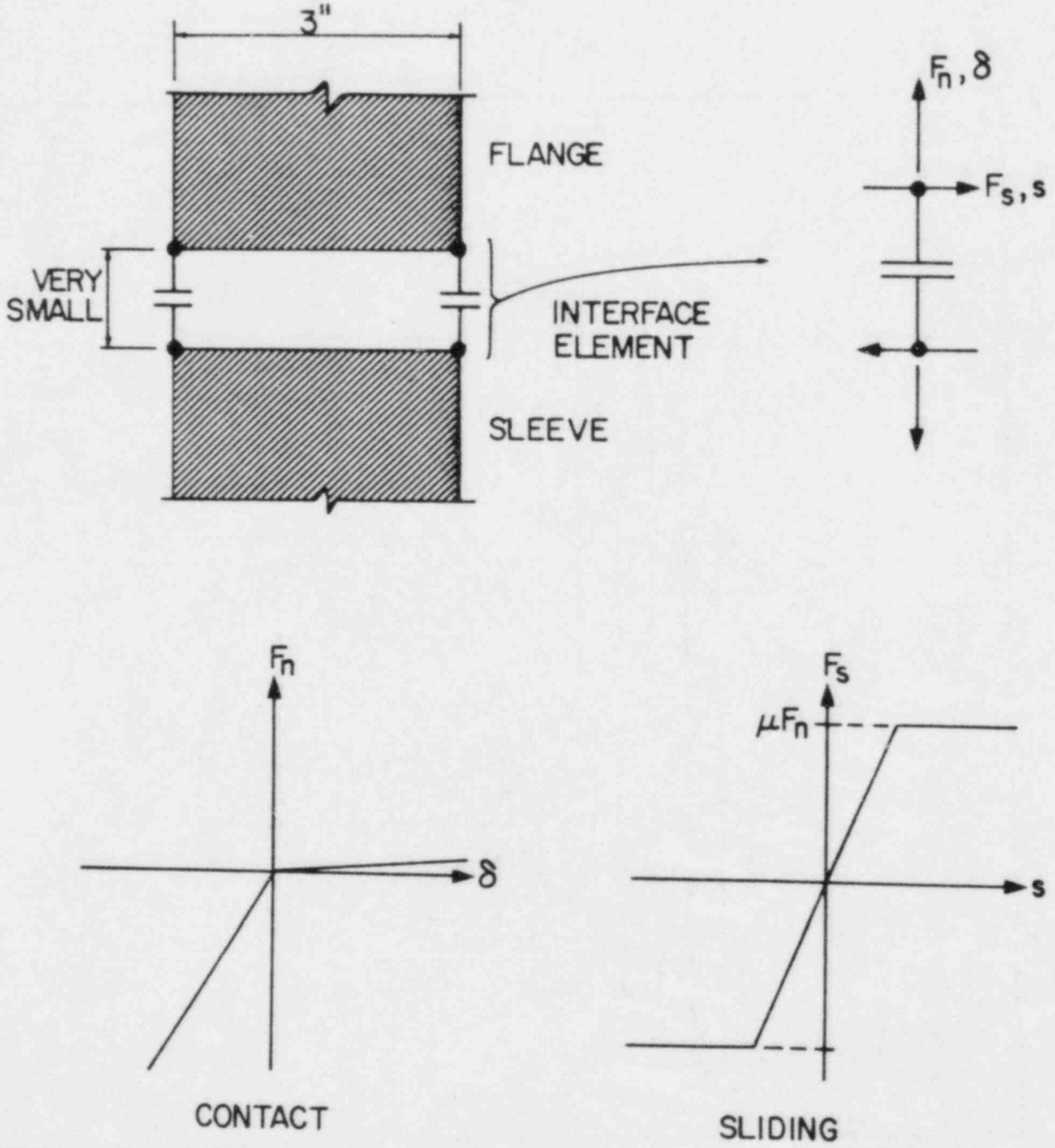

Figure 4.3 Flange/Sleeve Interface Idealization

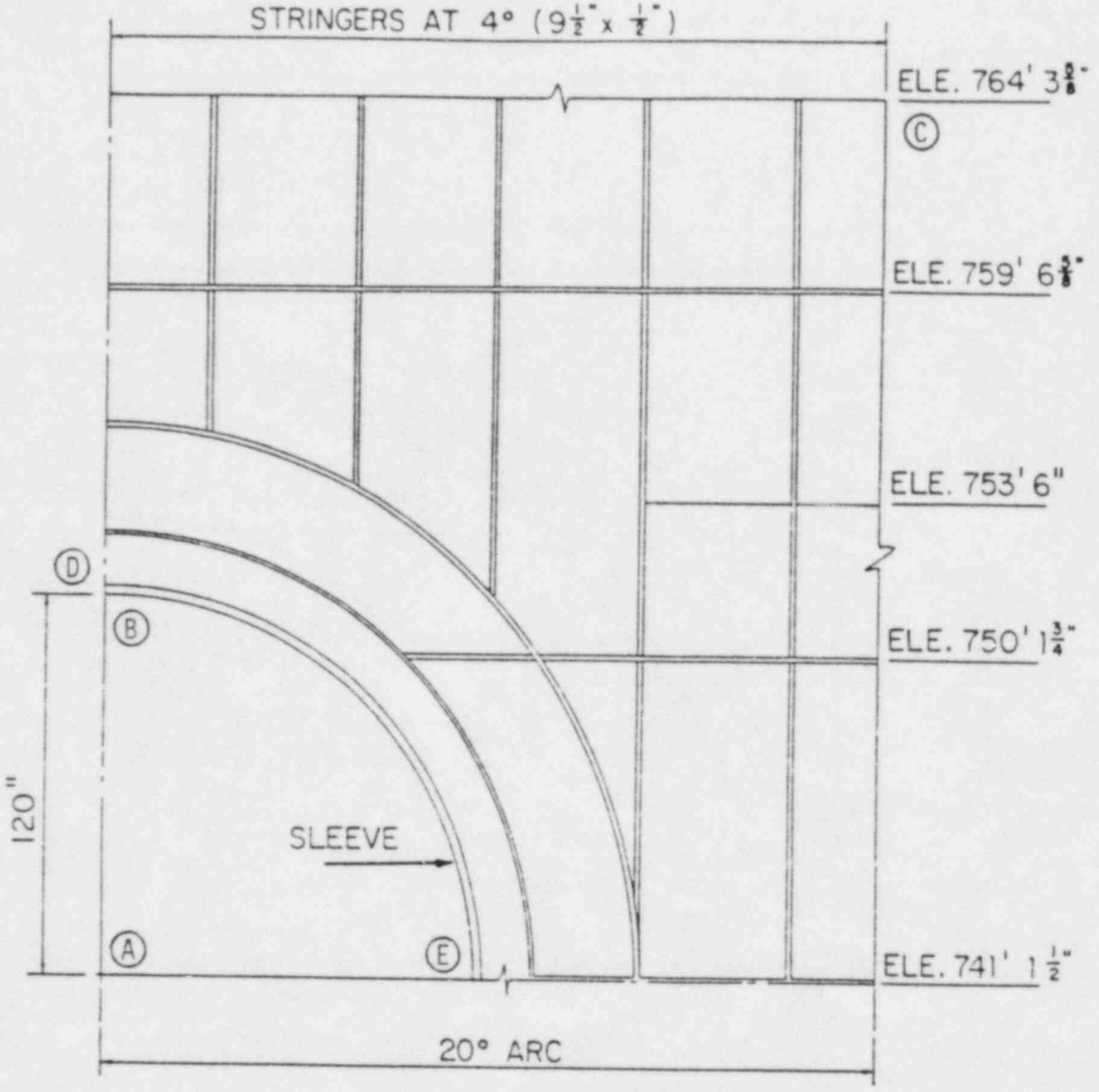

Figure 4.4 Sequoyah Containment Shell Reference Points (see also Figure 4.7 and 4.8)

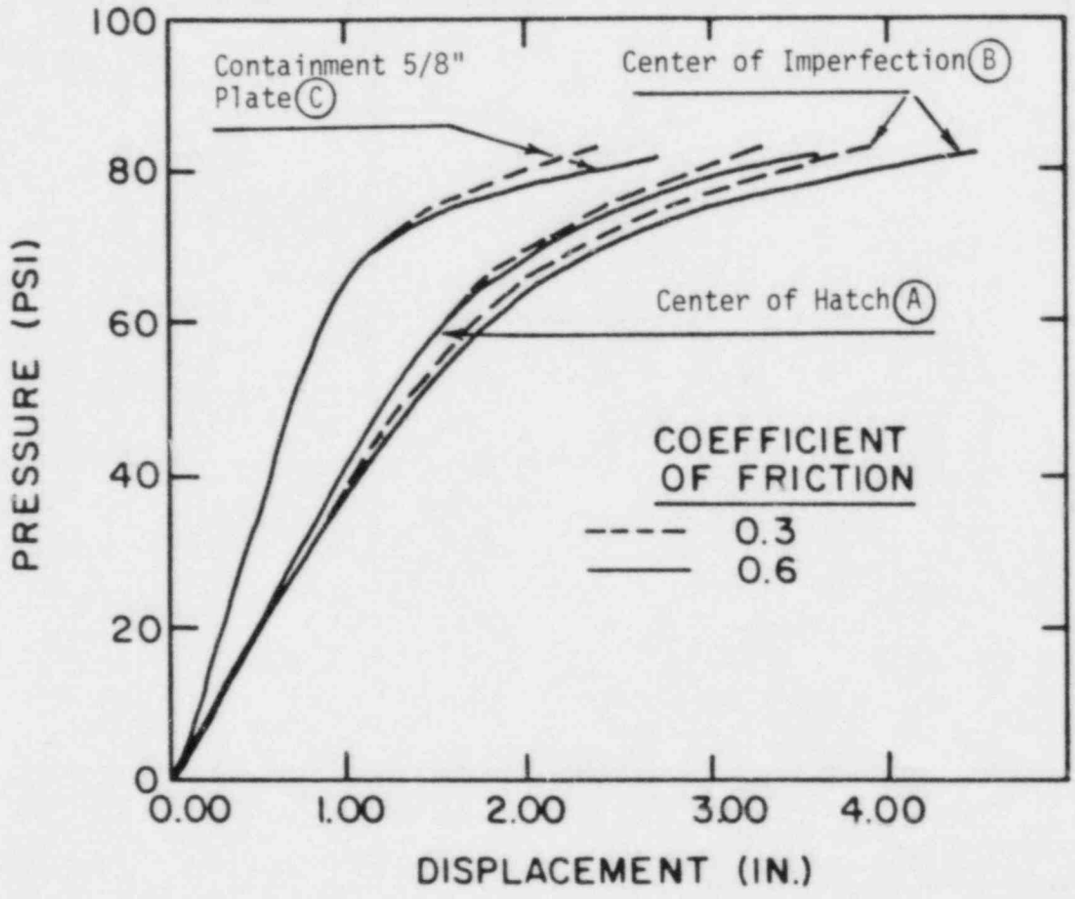

Figure 4.5 Radial Displacement

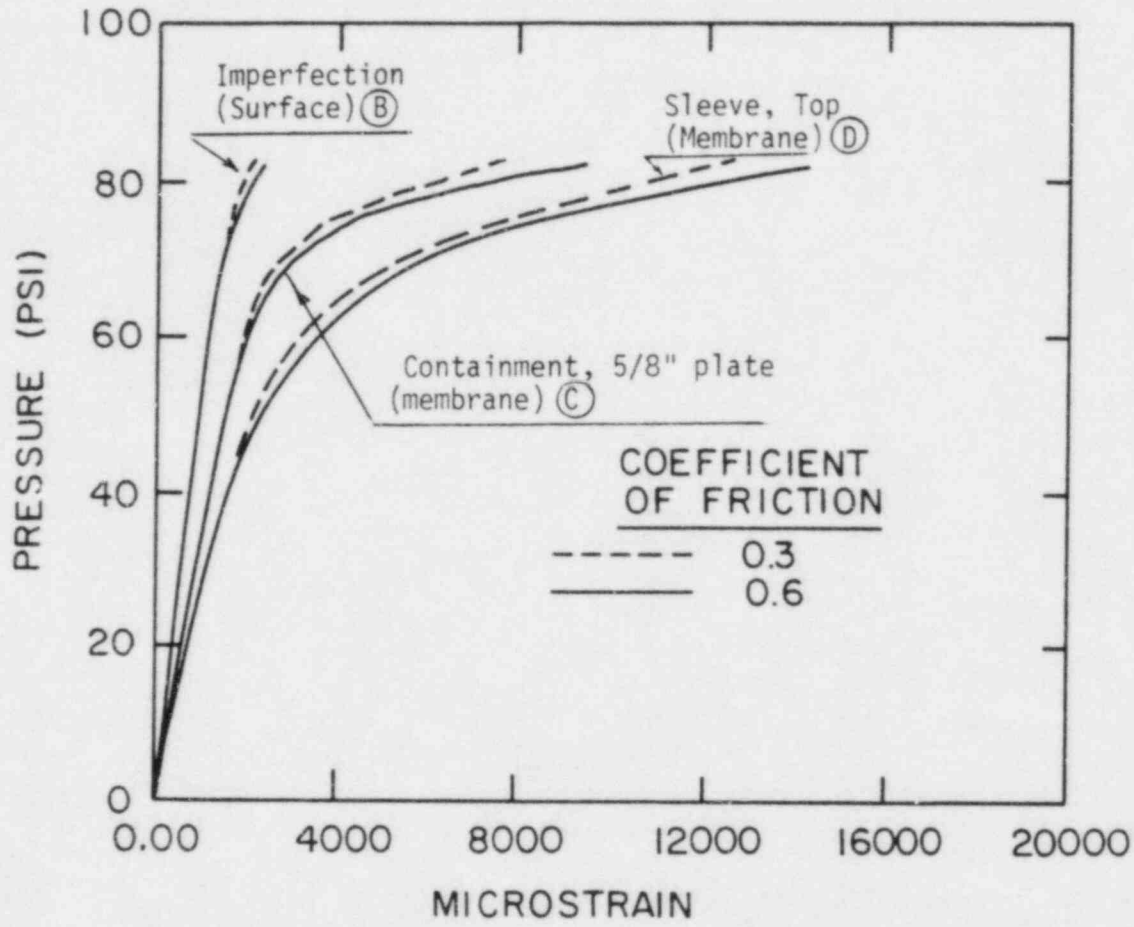

Figure 4.6 Strains at Selected Location in the Hatch Model

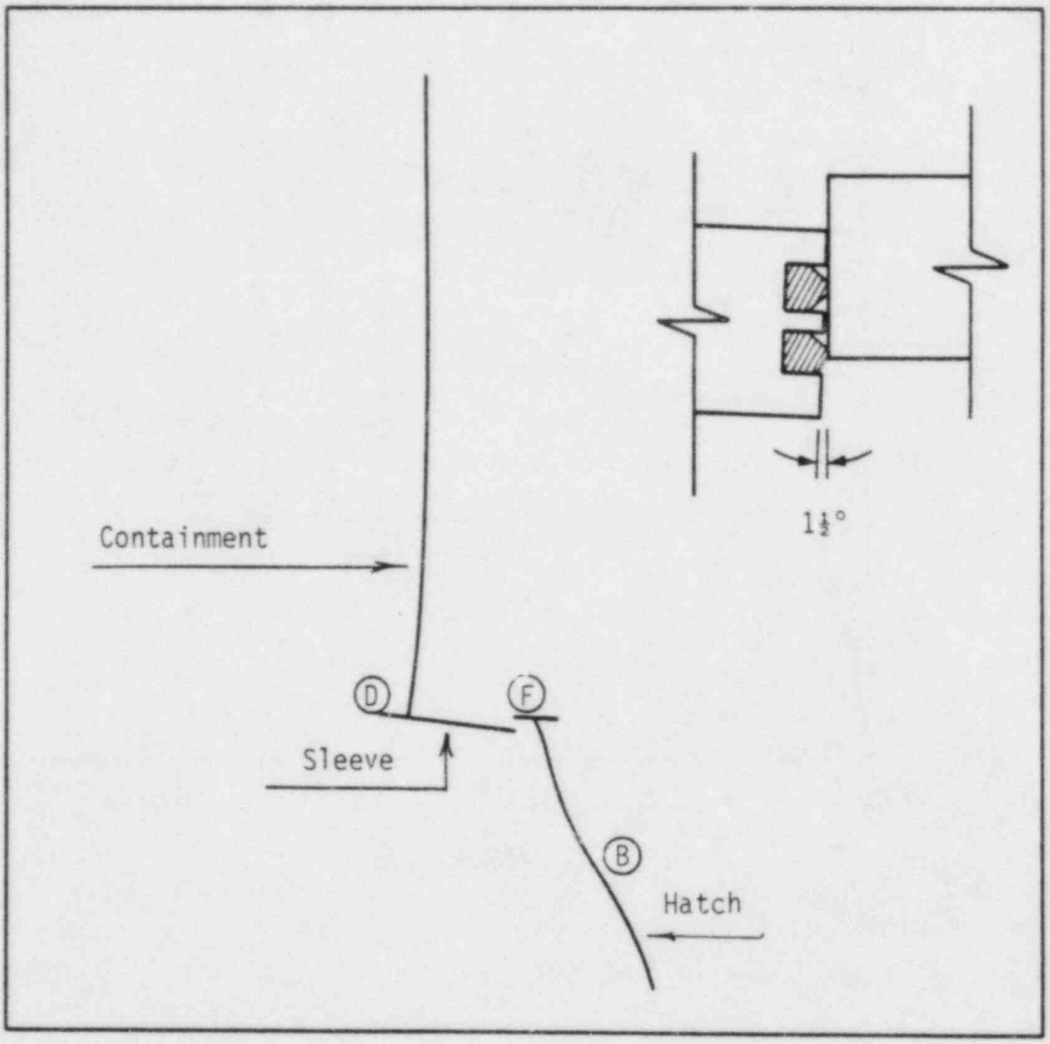

Figure 4.7 Displaced Shape in Vertical Symmetry Plane (82 psig, coefficient of friction = 0.3) (Displacement magnification equals 20 on left figure; equals 1.00 on inset.)

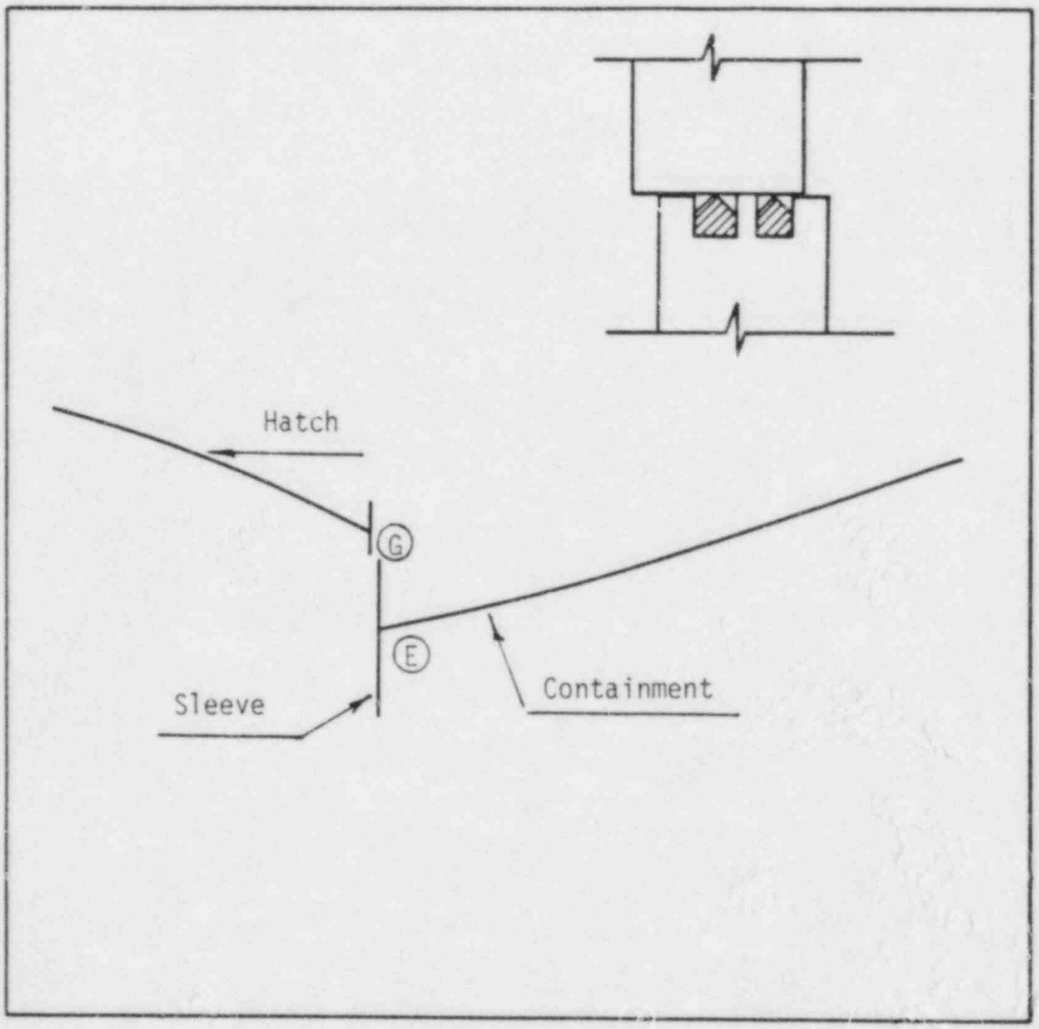

Figure 4.8 Displaced Shape in Horizontal Symmetry Plane (82 psig, coefficient of friction = 0.3) (Displacement magnification equals 20 on left figure; equals 1.00 on inset.)

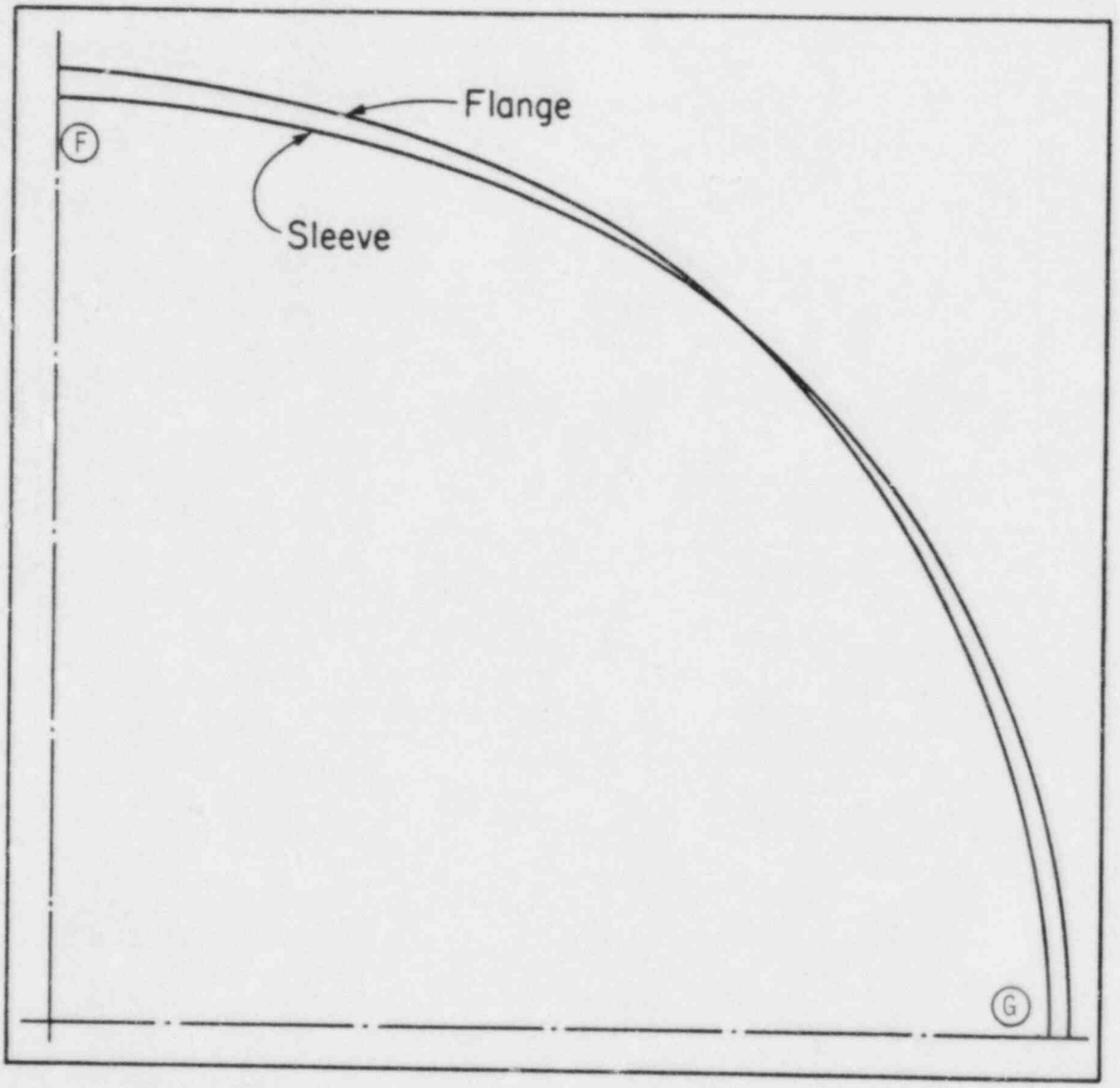

Figure 4.9 Flange/Sleeve Mismatch (82 psig, coefficient of friction = 0.3)
(Displacement magnification equals 20.)

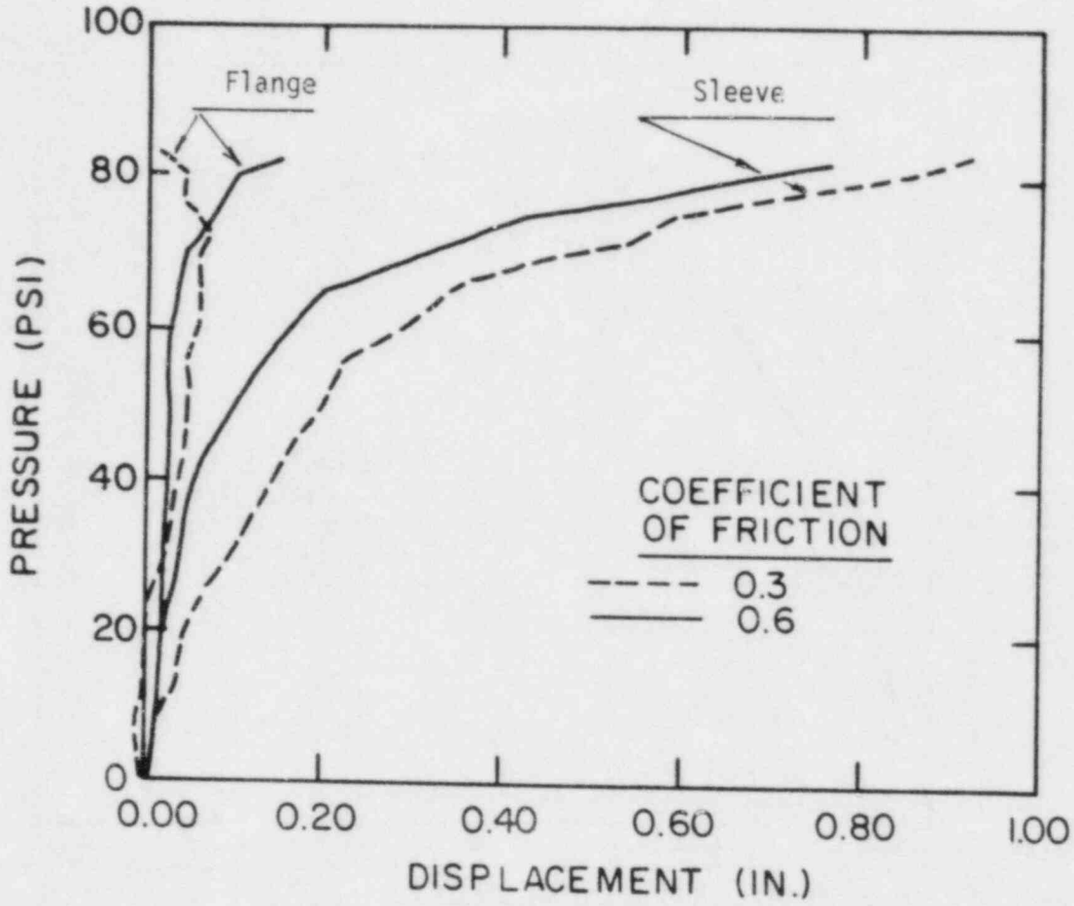

Figure 4.10 Radial Displacement at Seal Surface, Vertical Symmetry Plane, (F)

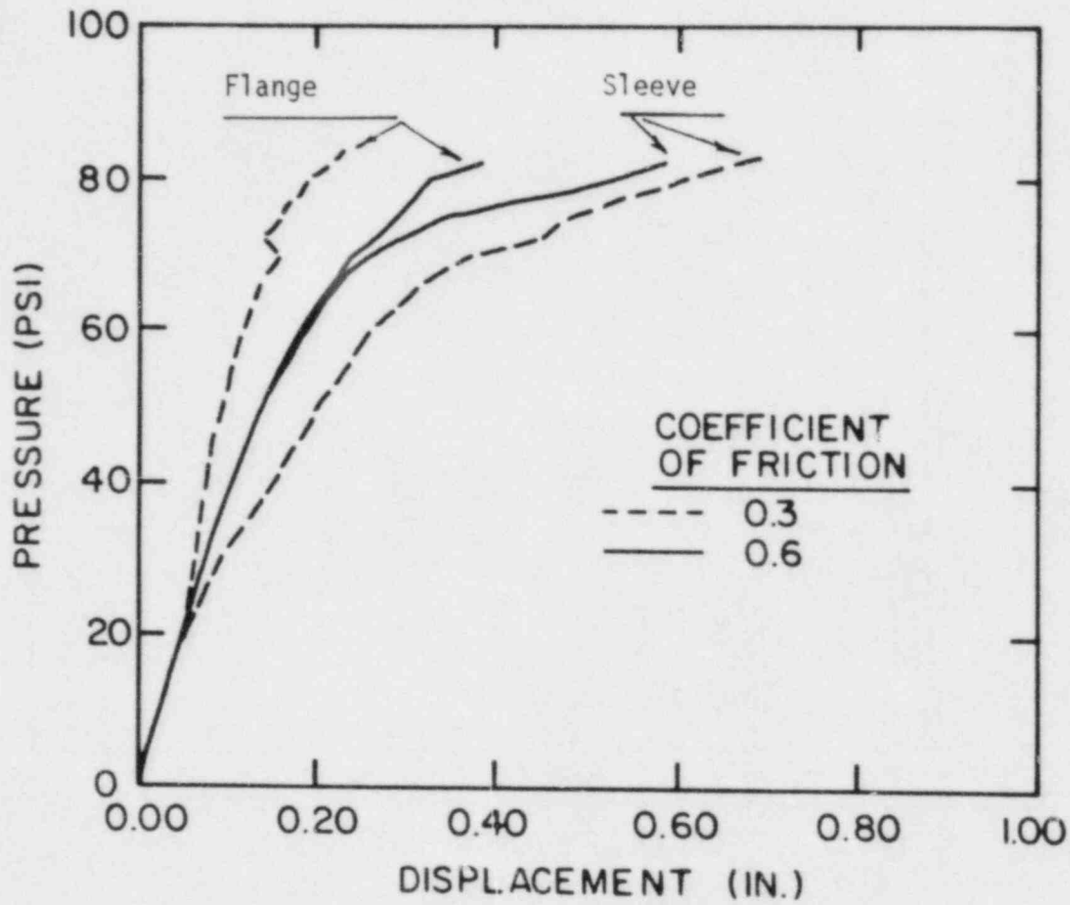

Figure 4.11 Radial Displacement at Seal Surface, Horizontal Symmetry Plane, (G)

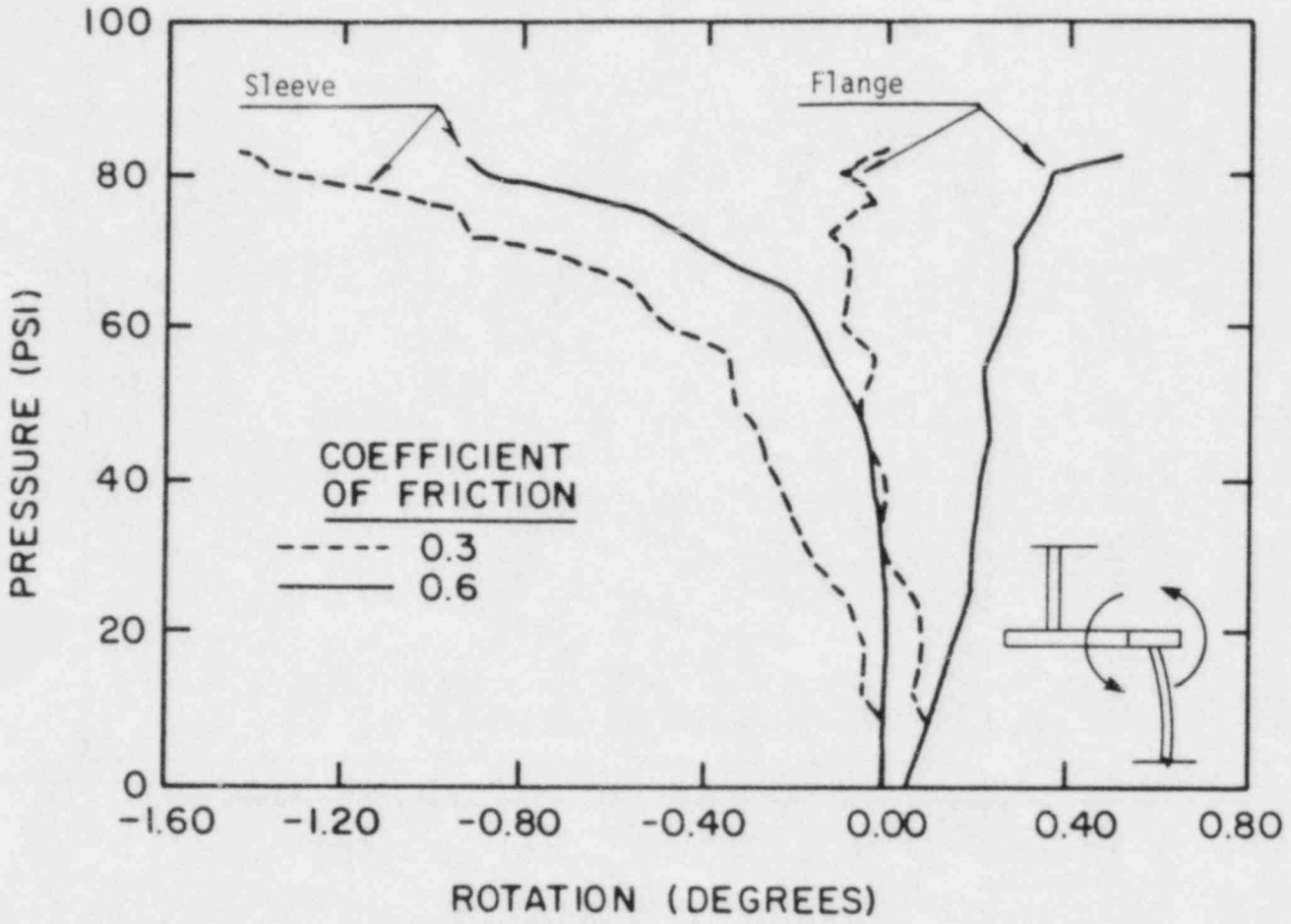

Figure 4.12 Rotation at Seal Surface, Vertical Symmetry Plane, (F)

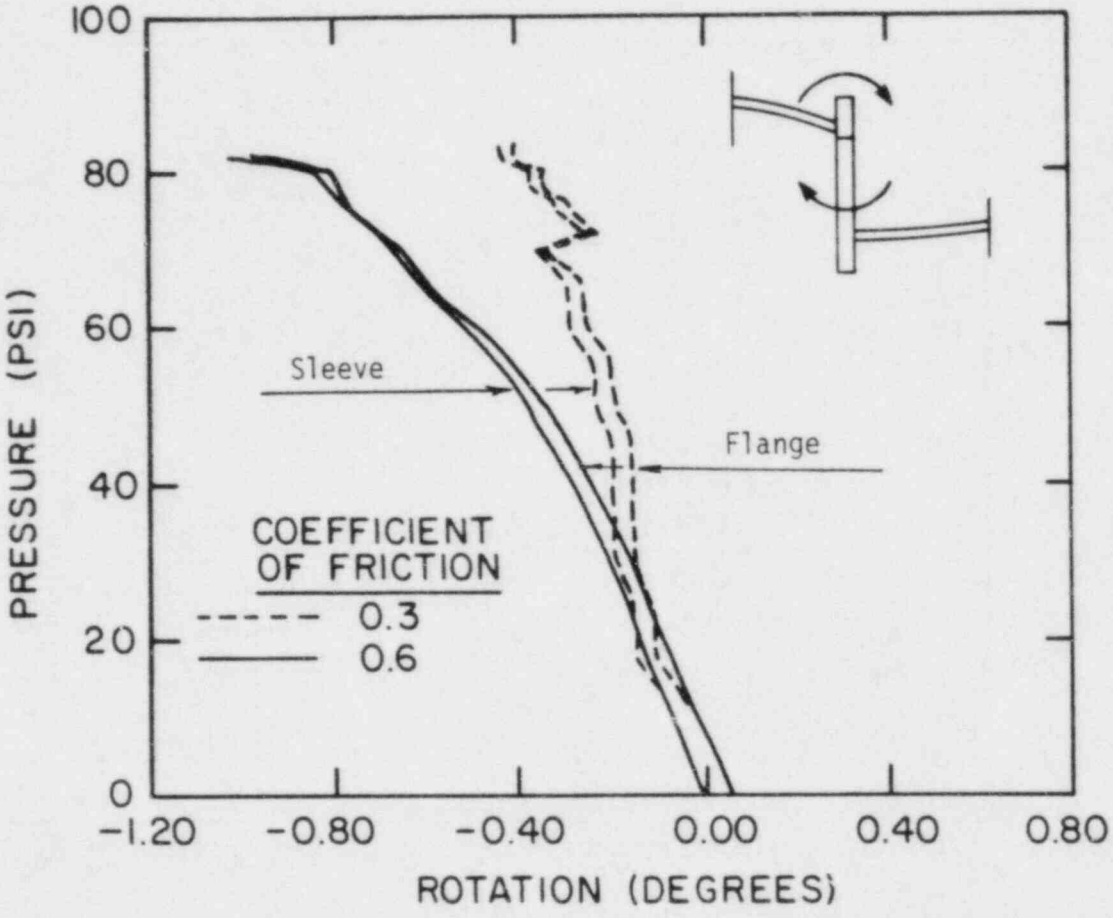

Figure 4.13 Rotation at Seal Surface , Horizontal Symmetry Plane , (G)

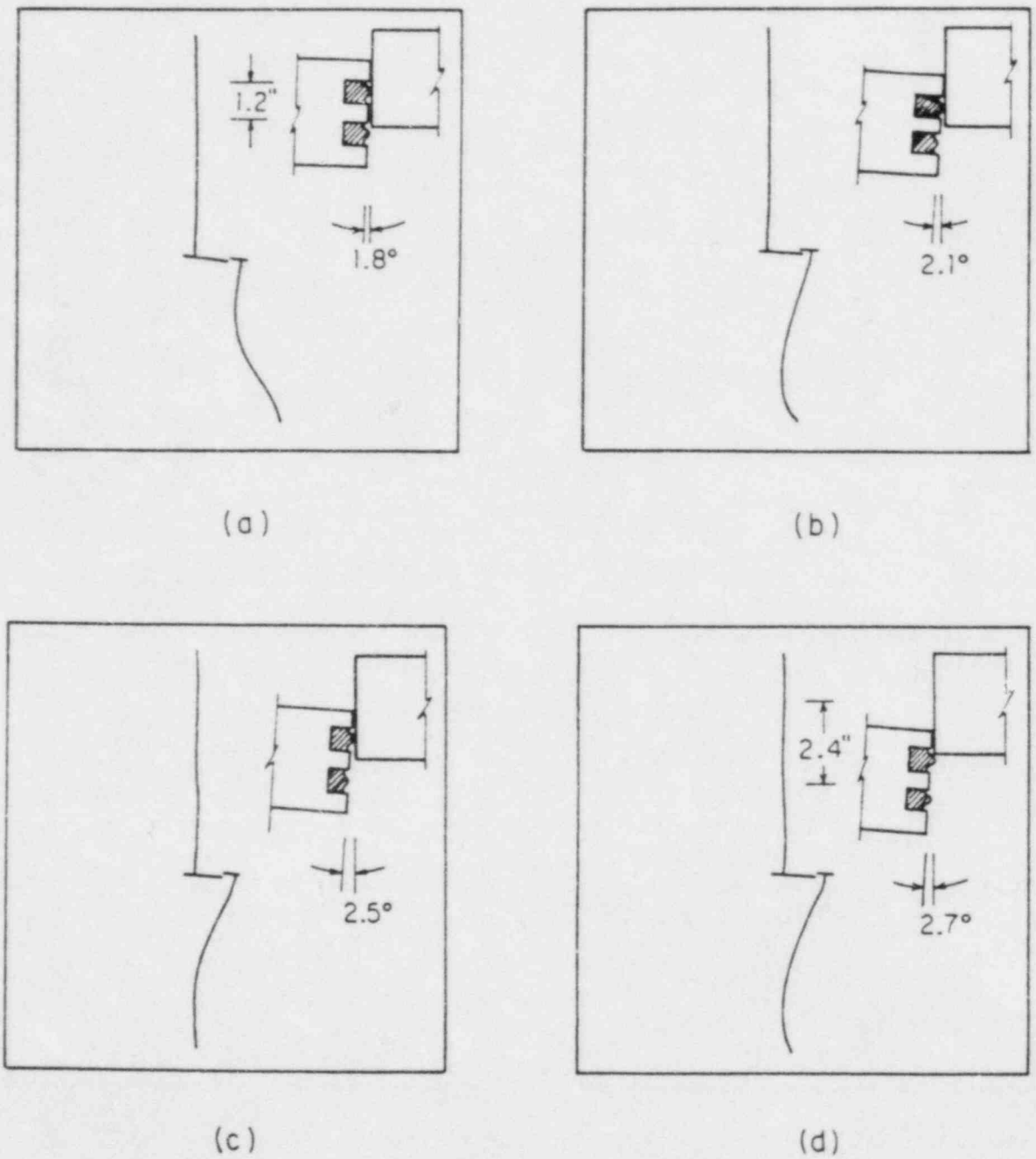

Figure 4.14 Displaced Shape at Different Stages During the Postbuckling Process at Vertical Symmetry Plane
(90 psig, coefficient of friction = 0.3)
(Displacement magnification equals 1.00)

NRC FORM 335 (2-84) NRCM 1102, 3201, 3202

U.S. NUCLEAR REGULATORY COMMISSION

BIBLIOGRAPHIC DATA SHEET

SEE INSTRUCTIONS ON THE REVERSE

1. REPORT NUMBER (Assigned by TIDC, add Vol. No., if any)
NUREG/CR-3952
IS-4862

2. TITLE AND SUBTITLE
Sequoyah Equipment Hatch Seal Leakage

3. LEAVE BLANK

4. DATE REPORT COMPLETED
MONTH: February YEAR: 1985

5. AUTHOR(S)
L. Greimann, P. Fanous and D. Bluhm

6. DATE REPORT ISSUED
MONTH: July YEAR: 1985

7. PERFORMING ORGANIZATION NAME AND MAILING ADDRESS (Include Zip Code)
Ames Laboratory
Iowa State University
Ames, IA 50011

8. PROJECT/TASK/WORK UNIT NUMBER

9. FIN OR GRANT NUMBER
FIN NO. A4135-4

10. SPONSORING ORGANIZATION NAME AND MAILING ADDRESS (Include Zip Code)
Division of Engineering
Office of Nuclear Reactor Regulation
U.S. Nuclear Regulatory Commission
Washington, D.C. 20555

11a. TYPE OF REPORT
Final (Technical)

b. PERIOD COVERED (Inclusive dates)

12. SUPPLEMENTARY NOTES

13. ABSTRACT (200 words or less)

Nuclear containments which will not leak significantly, that is, beyond technical specifications, during a design accident may leak severely during a severe accident when the pressure increases beyond the design level. Small leaks which are visualized as occurring at local details may occur before complete vessel failure. Buckling of the hatch door, large deformations and ovaling of the hatch sleeve are potential causes of mismatch at the sealing surface which can result in a leakage path. As a typical example of steel containments the Sequoyah equipment hatch was selected. If penetrations effects are neglected, gross yielding of the 1/2-inch shell plate near the springline of the Sequoyah containment will occur at an internal pressure of between 50 and 60 psi. The results of a finite element analysis showed that a maximum of 0.9 inch of relative sliding occurred at the seal interface at 82 psi and the maximum relative rotation was 1-1/2 degrees. The buckling load was predicted to occur in the range of 85 to 90 psi, far above gross yielding of shell. Although buckling increased the relative seal motions, they remained sufficiently small to prevent leakage. The Sequoyah equipment hatch should not leak before strains of several percent develop in the 1/2-inch containment shell plate near the springline, which occurs between 50 and 60 psi. In the unlikely event of hatch buckling, postbuckling deformations would not introduce leakage.

14. DOCUMENT ANALYSIS – a. KEYWORDS/DESCRIPTORS
Containment 01 Containment Shells Leaks

b. IDENTIFIERS/OPEN-ENDED TERMS

15. AVAILABILITY STATEMENT
Unlimited

16. SECURITY CLASSIFICATION
(This page) Unclassified
(This report) Unclassified

17. NUMBER OF PAGES

18. PRICE